Paleoenvironmental inferences on the Late Miocene hominoid-bearing site of Can Llobateres (NE Iberian Peninsula): An ecometric approach based on functional dental traits

Sara G. Arranz[a,*], Isaac Casanovas-Vilar[a], Indrė Žliobaitė[b,c], Juan Abella[d,a,e], Chiara Angelone[f,g], Beatriz Azanza[h], Raymond Bernor[i,j], Omar Cirilli[i,k], Daniel DeMiguel[h,l,a], Marc Furió[m,a], Luca Pandolfi[n], Josep M. Robles[a], Israel M. Sánchez[a], Lars W. van den Hoek Ostende[o], David M. Alba[a,*]

[a] *Institut Català de Paleontologia Miquel Crusafont, Universitat Autònoma de Barcelona, c/ Columnes s/n, 08193 Cerdanyola del Vallès, Barcelona, Spain*

[b] *Department of Computer Science, University of Helsinki, P.O. Box 68, 00014 Helsinky, Finland*

[c] *Department of Geosciences and Geography, University of Helsinki, P.O. Box 64, 00014 Helsinky, Finland*

[d] *Grup d'Investigació en Paleontologia de Vertebrats del Cenozoic (PVC-GIUV), Departament de Botànica i Geologia, Universitat de València, 46100 Burjassot, València, Spain*

[e] *Instituto Nacional de Biodiversidad (INABIO), Pje. Rumipamba N. 341 y Av. de los Shyris (Parque La Carolina), Quito, Ecuador*

[f] *Dipartimento di Scienze, Universita` degli Studi Roma Tre, 00146 Roma, Italy*

[g] *Key Laboratory of Vertebrate Evolution and Human Origins, Institute of Vertebrate Paleontology and Paleoanthropology, Chinese Academy of Sciences, 100044 Beijing, China*

[h] *Departamento de Ciencias de la Tierra, and Instituto Universitario de Investigación en Ciencias Ambientales de Aragón (IUCA), Universidad de Zaragoza, 50009, Zaragoza, Spain*

[i] *College of Medicine, Department of Anatomy, Laboratory of Evolutionary Biology, Howard University, 520 W St. N.W., 20059, Washington D.C., USA*

[j] *Human Origins Program, Department of Anthropology, National Museum of Natural History, Smithsonian Institution, 20013, Washington DC, USA*

[k] *Earth Sciences Department, Paleo[Fab]Lab, Università degli Studi di Firenze, via G. La Pira 4, I-50121, Firenze, Italy*

[l] *ARAID foundation, 50018, Zaragoza, Spain*

[m] *Serra Húnter Fellow, Departament de Geologia, Universitat Autònoma de Barcelona, Campuys de la UAB, 08193 Cerdanyola del Vallès,, Barcelona, Spain*

[n] *Dipartimento di Scienze, Università della Basilicata, via dell'Ateneo Lucano, 10, 85100, Potenza, Italy*

[o] *Naturalis Biodiversity Center, Darwinweg 2, 2333 CR Leiden, The Netherlands*

***Corresponding authors.**

E-mail addresses: sara.arranz@icp.cat (S.G. Arranz); david.alba@icp.cat (D.M. Alba).

Paleoenvironmental inferences on the Late Miocene hominoid-bearing site of Can Llobateres (NE Iberian Peninsula): An ecometric approach based on functional dental traits

Abstract

Hispanopithecus laietanus from the Late Miocene (9.8 Ma) of Can Llobateres 1 (CLL1; Vallès-Penedès Basin, NE Iberian Peninsula) represents one of the latest occurrences of fossil apes in Western mainland Europe, where they are last recorded at ~9.5 Ma. The paleoenvironment of CLL1 is thus relevant for understanding the extinction of European hominoids. To refine paleoenvironmental inferences for CLL1, we apply ecometric models based on functional crown type (FCT) variables—a scoring scheme devised to capture macroscopic functional traits of occlusal shape and wear surfaces of herbivorous large mammal molars. Paleotemperature and paleoprecipitation estimates for CLL1 are provided based on published regional regression models linking average FCT of large herbivorous mammal communities to climatic conditions. A mapping to Whittaker's present-day biome classification is also attempted based on these estimates, as well as a case-based reasoning via canonical variate analysis of FCT variables from five relevant biomes. Estimates of mean annual temperature (25 °C) and mean annual precipitation (881 mm) classify CLL1 as a tropical seasonal forest/savanna, only in partial agreement with the canonical variate analysis results, which classify CLL1 as a tropical rainforest with a higher probability. The former biome agrees better with previous inferences derived from fossil plants and mammals, as well as preliminary isotopic data. The misclassification of CLL1 as a tropical forest is attributed to the mixture of forest-adapted taxa with others adapted to more open environments, given that faunal and plant composition indicates the presence of a dense wetland/riparian forest with more open woodlands nearby. The tested FCT ecometric approaches do not provide unambiguous biome classification for CLL1. Nevertheless, our results are consistent with those from other

approaches, thus suggesting that FCT variables are potentially useful to investigate paleoenvironmental changes through time and space—including those that led to the extinction of European Miocene apes.

Key words: Fossil apes; *Hispanopithecus*; Functional crown types; Paleoecology; Vallesian; Spain.

1. Introduction

1.1. The hominoid-bearing site of Can Llobateres

Historical background The fossil site of Can Llobateres (Late Miocene), in the municipality of Sabadell (Catalonia, NE Spain), has figured prominently in the study of Miocene mammals from Europe—being considered the reference locality of MN9 (Mein, 1990)—with emphasis on fossil hominoids. The site was discovered in 1926 (Crusafont Pairó, 1969; Alba et al., 2011a, 2011b) and the first accounts of its fauna were published in the 1940s (Villalta Comella and Crusafont Pairó, 1943; Crusafont Pairó and Villalta Comella, 1948). Hominoid dental remains, assigned to the dryopithecine[1] *Hispanopithecus laietanus*, were first discovered there in 1958 (Crusafont Pairó, 1958; Crusafont Pairó and Hürzeler, 1969) and additional hominoid remains were subsequently recovered during the 1960s (Crusafont Pairó and Hürzeler 1961, 1969; Crusafont Pairó 1965; Golpe Posse 1982, 1993; Moyà-Solà et al. 1990). Crusafont and Hürzeler (1961, 1969) reported two additional species from the site—never figured or described, and

[1] Although it is currently uncertain whether the Dryopithecinae constitute a clade or a paraphyletic assemblage (Alba, 2012; Almécija et al., 2021; Pugh, 2022), we follow Urciuoli and Alba (2023) in provisionally distinguishing this group at the subfamily rank until its phylogenetic relationships are clarified further.

hence considered nomina nuda (Szalay and Delson, 1979; Alba, 2012; Alba et al., 2012a)—while a fourth hominoid was subsequently reported based on an isolated male upper canine (Crusafont Pairó and Golpe Posse, 1973), being attributed to *Sivapithecus indicus*.

In 1981, additional dental hominoid material was recovered from the lower levels of the site (Begun et al., 1990; Golpe Posse, 1993), known as Can Llobateres 1 (CLL1). From 1992 onward, a partial cranium (Moyà-Solà and Köhler, 1993, 1995; Begun, 1994) and skeleton (Moyà-Solà and Köhler, 1996; Almécija et al., 2007; Pina et al., 2012; Tallman et al., 2013; Susanna et al., 2014) were discovered on the upper levels of the site, termed Can Llobateres 2 (CLL2), which were last excavated in 1997. In 2010, excavations were resumed again at CLL1 by a team led from the Institut Català de Paleontologia Miquel Crusafont (ICP) and additional hominoid teeth were found (Alba et al., 2012a), along with plant remains that enabled a better characterization of the paleoenvironment (Marmi et al., 2012). The locality of CLL1 was last excavated in 2015, owing to the paucity of the fossiliferous levels that delivered most of the hominoid dental remains in previous years. Begun et al. (1990) and most subsequent authors attributed the whole hominoid sample from Can Llobateres to *Dryopithecus laietanus* (Harrison, 1991; Moyà-Solà and Köhler, 1993, 1995, 1996; Begun, 1994; Ribot et al., 1996) or, more recently, *Hispanopithecus laietanus* (Almécija et al., 2007; Cameron, 1997, 1998, 1999, 2004; Moyà-Solà et al., 2009; Begun, 2009; Alba, 2012; Alba et al., 2012a).

Geological background and taphonomical remarks Can Llobateres is located in the Vallès sector of the Vallès-Penedès Basin (Catalonia, Spain; Fig. 1), an elongated half-graben about 100 km in length and 12–14 km in width, parallel to the Catalan coastline near Barcelona, and bounded by the Catalan Coastal Ranges (for an updated review, see Casanovas-Vilar et al., 2016a). The Miocene sedimentary infill of the Vallès-Penedès Basin has been divided into four main litostratigraphic units, Can Llobateres belonging to the Upper Continental Units, which range from the Middle to the Late Miocene (Casanovas-Vilar et al., 2016a). In particular, Can

Llobateres is located within distal facies of the alluvial fan system of Castellar del Vallès (Agustí et al., 1996, 1997), consisting of a short sequence ~20 m thick mostly defined by mudstones (claystones and siltstones), as well as polymictic breccias and conglomerates (Marmi et al., 2012; Alba et al., 2012a). The locality of CLL1 is located in the lower section of the sequence, characterized by organic matter and abundant mudstones, indicating a poorly drained alluvial plain that would have favored the development of small shallow lakes and ponds (Agustí et al., 1996; Alba et al., 2011a, 2011b, 2012a).

No taphonomic study has been performed at CLL1, but Begun et al. (1990) made some sedimentological and taphonomic remarks based on the 1981 campaign, while Marmi et al. (2012) and Alba et al. (2012a) provided far more detailed sedimentological descriptions and additional taphonomic details based on the 2010–2011 campaigns. The former authors distinguished two 'sedimentary units' at CLL1, which they interpreted as corresponding to two different 'fluvial cycles' (Begun et al., 1990): the lower one, characterized by finer sediments indicative of a low energy depositional environment, would have yielded taxa associated with humid and forested environments (such as primates and suids); the upper one, in turn, would be characterized by coarser sediments (including channel deposits) indicative of a higher energy depositional environment and, according to these authors, would have yielded taxa indicative of more open conditions (such as hipparionin equids) that could have been transported from greater distances. Subsequent fieldwork at the site (Alba et al., 2012a) confirmed that primates are apparently restricted to the lower 'unit' recognized by Begun et al. (1990), but evinced a greater stratigraphic and taphonomic complexity (Alba et al., 2012a; Marmi et al., 2012), in which four stratigraphic bodies may be discerned.

The bottom of the CLL1 sequence (not available to Begun et al., 1990) is composed by layers of reddish to brown silts, sands, and conglomerates, indicative of less humid conditions than the 'classical' layers of CLL1, probably representing the end of a preceding depositional cycle

(Alba et al., 2012a). The lower 'unit' of Begun et al. (1990), in turn, comprises variously colored mudstones (mostly fine-grained clays) with abundant micromammal and some macromammal remains (including the hominoid teeth recovered in 1981 and 2011), plus mollusk shells, silicified figs, and other fragmentary and poorly preserved plant remains. The lower layers (1a and 1b) are blackish and become lighter in color (ligh gray to greenish) toward the top (layer 2), although at different locations layers 1b and 2—the ones that yielded primate remains—are completely light brown (Alba et al., 2012a; Marmi et al., 2012). The top layers (3a and 3b) consist of greenish to yellowish clays with some coarser sediments, in which gastropod shells are poorly preserved and vertebrate remains sparser than in the underlying layers. The upper 'unit' of Begun et al. (1990) begins with a paleochannel (layer 4a) of varying thickness composed of much coarser sediments (with decreasing granulometry from bottom to top), which at some point erodes some or all of the aforementioned layers and which locally yielded more abundant large mammal remains. Overlying these channel deposits there is a thick (>2.5 m) sedimentary package (layer 4b/4p) of alternating green clays, greenish to orange silts, and conglomerates, which locally preserve abundant plant macroremains (Marmi et al., 2012). A fourth sedimentary body can be distinguished at the top of the CLL1 sequence, including a paleochannel (layer 5a) that erodes layer 4b and an overlying 6.5 m-thick package (layer 5b) of multiple episodes of ocher to red clays, silts, and conglomerates, indicative of paleosol formation and well-aerated conditions (Marmi et al., 2012).

Pending more detailed analyses, and contrary to Begun et al.'s (1990) previous assessment, the 2010–2015 fieldwork campaigns (D.M.A., pers. obs.) failed to confirm differences in faunal composition between the primate-bearing layers and the paleochannel deposits (other than the apparent lack of primates in the latter). For example, suids are not restricted to the primate-bearing layers (contra Begun et al., 1990) but also present in the paleochannel deposits (layer 4a) and in the layer 4b that overlies them. Similarly, *Hippotherium* remains are more abundant

121 in layer 4a, but are also present in most of the remaining layers, both above (4b) and below (3b,
122 2, and 1b), thus including the primate-bearing ones. Finally, that forest-adapted taxa are not
123 restricted to the latter is best exemplified by the recovery of a *Tapirus* tooth from the bottom of
124 layer 4a (D.M.A., pers. obs.). Coupled with the fact that detailed stratigraphic provenance is
125 not recorded for most of the remains recovered before 2010, this makes impossible to
126 conclusively ascertain whether, in fact, CLL1 as a whole mixes faunal elements from different
127 environments due to differential transport among various fossiliferous layers.

128 On the other hand, different degrees of transport depending on the layer are confirmed by
129 available data. In particular, the presence of isolated teeth from two single individuals
130 (hominoid and cervid) scattered over a few square meters in one of the clay layers that yielded
131 primate remains suggests minimal transport, probably under water (Alba et al., 2012a). By
132 contrast, the paleochannel combines fragmentary and rounded remains of multiple large
133 mammals with better preserved and larger macromammal remains (incluing disarticulated
134 dentognathic and postcranial remains of a single *Hippotherium* individual; D.M.A., pers.
135 obs.)—overall indicative of transport in higher energy conditions from longer distances, than
136 in the primate-bearing layers as previously concluded by Begun et al. (1990). Finally, the plant
137 remains from layer 4p (Marmi et al., 2012) are interpreted as a parautochtonous assemblage
138 acumulated by wind and short water transport in a shallow-water epositional environment. All
139 this preliminary taphonomic evidence combined suggests that the fossil assemblages from
140 CLL1 are representative of the fauna and flora present at and near the depositional environment,
141 although it cannot be discounted that some taxa preferentially inhabited areas farther away from
142 it, as some fossiliferous layers evince greater degrees of transport than others.

143 Chronological and paleoenvironmental background On biostratigraphic grounds, CLL1 is
144 correlated to the *Cricetulodon hartenbergeri–Progonomys hispanicus* interval local subzone,
145 while CLL2 is correlated to the *Cricetulodon sabadellensis* + *Progonomys hispanicus*

concurrent range local subzone (Casanovas-Vilar, 2016b). In addition, the Can Llobateres sequence records three magnetozones, with reverse polarity in the lower and upper part, and normal polarity in the middle (Agustí et al., 1996, 1997). In particular, CLL1 is correlated to C4Ar.3r while CLL2 is correlated to C4Ar.2r (Agustí et al., 1996, 1997), with interpolated ages of 9.76 and 9.62 Ma, respectively (Casanovas-Vilar et al., 2016b). Based on the absence of *Progonomys* from CLL1, it has traditionally been considered that the Can Llobateres sequence records the early to the late Vallesian transition, with CLL1 and CLL2 being correlated to MN9 and MN10, respectively (Agustí et al., 1996, 1997; Alba et al., 2012a); indeed, CLL1 is considered the reference locality for MN9 (Mein, 1990; de Bruijn et al., 1992; Casanovas-Vilar et al., 2016b). However, *Progonomys* remains have been found in older sites from other Iberian basins, placing the lower boundary of MN10 (as defined by the first common occurrence of this genus) at 9.98 Ma (Hilgen et al., 2012; Van Dam et al., 2014). Accordingly, under a strictly biostratigraphic approach to MN units, CLL1 must be correlated to MN10 instead of MN9 (Casanovas-Vilar et al., 2016b; Alba et al., 2018). It is unlikely that the paleobiodiversity of CLL1 is inflated by time averaging, as most of the remains come from a short stratigraphic interval of ~2 m (Alba et al., 2012a). Based on the average sedimentation rate for the Vallesian of the Vallès-Penedès Basin (20 cm/kyr; Garcés et al., 1996) this would merely represent a time interval of ~10 kyr—in rough agreement with the difference between the interpolated ages of CLL1 and CLL2 (~140 kyr; Casanovas-Vilar et al., 2016b), which are separated by less than 20 m of stratigraphic distance.

Paleoenvironmental inferences have previously been drawn for CLL1 based on both mammals and plants, using different methods—see summary in Table 1 and the Discussion for additional details. The plant remains (Sanz de Siria Catalán, 1993, 1994; Álvarez Ramis, 1975; Alba et al., 2011b; Marmi et al., 2012), which enable a reliable reconstruction of the paleoenvironment that *H. laietanus* inhabited, are generally in agreement with the conclusions

drawn from the large and/or small mammals (Nagatoshi, 1987; Köhler, 1993; Andrews, 1996; Hernández Fernández et al., 2003; Casanovas-Vilar and Agustí, 2007; Costeur, 2005), which indicate the presence of a humid and closed forest paleoenvironment at the depositional area but further hint at the existence of relatively more open woodlands nearby (Marmi et al., 2012). Some paleoenvironmental conclusions have also been derived for CLL1 from the numerical analyses of its mammalian assemblage composition (Andrews, 1996; Hernández Fernández et al., 2003) and ecometrics in general have been applied to this site as part of studies that aimed to reconstruct continental patterns of Neogene paleoprecipitation (Fortelius et al., 2002; Eronen et al., 2009, 2010a; Kaya et al., 2018) or net primary production (Toivonen et al., 2022). However, no dedicated ecometric approaches to paleoenvironment reconstruction have been performed thus far. Given that *H. laietanus* is the latest hominoid recorded from mainland Western Europe, the reconstruction of its paleoenvironment is highly significant for understanding the local extinction of hominoids and other mammalian taxa in Europe during the Late Miocene (Casanovas-Vilar et al., 2011).

1.2. Ecometrics and functional crown types

Ecometrics is a trait-based approach based on the study of functional morphological features of organisms that attempts to quantify links between the distribution of those traits across biotic communities and specific environmental factors as well as to analyze their dynamics through space and time in the fossil record (Fortelius et al., 2002; Eronen et al., 2010b; Vermillion et al., 2018). Ecometric traits are measurable macroscopic features that are known to represent their function in relation to local environmental conditions (Eronen et al., 2010b)—either due to adaptive reasons or to use/plasticity (ecophenotypic features). The most typical ecometric traits of vertebrates describe dental morphology, limb proportions, and body mass. Candidate traits for ecometric modeling must be at least preliminarily known to be associated through

196 their functional relationship with the local environmental conditions, including the dominant
197 temperature, precipitation, or dominant vegetation type (Eronen et al., 2010b; Vermillion et al.,
198 2018). However, the exact associations are captured computationally when fitting statistical
199 models to link the traits of communities with their environmental conditions. Due to its
200 functional perspective, ecometrics has sometimes been referred to as a taxon-free approach, to
201 highlight that the ecology of fossil organisms is not inferred from that of their nearest living
202 relatives and that ecometric approaches do not rely on presence or absence of any particular
203 individual taxa. Theoretically, ecometric approaches can be completely taxon blind—e.g.,
204 analyzing random samples of teeth that are found at localities without considering any
205 taxonomic information. However, in practice, for robustness and potentially larger samples,
206 most ecometric studies, including the present work, analyze the distribution of traits over
207 species at localities, sometimes on global scale datasets (e.g., Liu et al., 2012; Žliobaitė et al.,
208 2018). Ecometrics, thus, does not focus on individual organisms, but deals with the functional
209 composition of communities, thereby enabling comparisons between present and past
210 communities. Of course, there is no way to statistically test for predictions about the past
211 (retrodictions), which makes it necessary to use different approaches and see how they compare.
212 Because of its relatively fast and non-destructive sampling, dental ecometrics has been
213 particularly used to make large-scale inferences about paleoenvironmental and biotic changes
214 across different geographic and temporal scales, and different tailored global and regional
215 models have been developed for different types of analysis (Eronen et al., 2010b; Liu et al.,
216 2012; Fortelius et al., 2016; Žliobaitė et al., 2016; Oksanen et al., 2019).
217 In this study, we aim at predicting multiple climatic characteristics of CLL1, for which we
218 use the dental trait scoring scheme reported in Žliobaitė et al. (2016), termed functional crown
219 types (FCT). This scheme was devised to potentially increase the scope of environmental
220 predictions particularly in the Late Miocene and Plio-Pleistocene. The scheme is based on a

modular system called crown types (Jernvall, 1995), which was designed to be applicable to mammals generally, primarily focusing on the shape of unworn teeth. Functional crown types, in contrast, focus on characteristics of how teeth wear while in use. The FCT scheme includes seven variables (Žliobaitė et al., 2016; Galbrun et al., 2018). Ecometric approaches based on hypsodonty (HYP; relative crown height) and loph count (Fortelius et al., 2002, 2016; Eronen et al., 2010a, 2010c; Liu et al., 2012; Oksanen et al., 2019) have been used to estimate paleoprecipitation and productivity in the Old World from the Miocene through the Pleistocene, as well as temperature in the Pleistocene. However, the set of seven variables of the FCT scheme offers potential for estimating a broader set of climatic conditions, including seasonality characteristics and reoccuring extremities of climatic conditions (Žliobaitė et al., 2016). Here, we apply regional and global ecometric approaches based on the FCT of herbivorous large mammals from CLL1 to refine the previous paleoenvironmental inferences on the habitat of *H. laietanus*.

2. Materials and methods

2.1. Studied material

As in Žliobaitė et al. (2016), this study was restricted to herbivorous large mammals of the orders Artiodactyla, Perissodactyla, Proboscidea, and Primates, and focused on M^2s (see also Galbrun et al., 2018). We scored dental traits at the species level. An updated faunal list of the mammals recorded at CLL1, including 20 species of the aforementioned orders (Table 2), was compiled based on the information available from the Vallès-Penedès Miocene Vertebrates – Paleobiodiversity Database (Casanovas-Vilar et al., 2018; Alba et al., 2022a), which includes specimen identification and provenance information for Miocene vertebrate remains from the Vallès-Penedès Basin and is maintained by ICP researchers, not yet openly accessible. The identification of multiple species was also revised in the course of this work by examining

246 original material housed in the ICP and comparing it with that from published sources.
247 Functional crown type variables were scored by visual inspection from M^2s in all species of
248 large herbivorous mammals. Žliobaitė et al. (2016) scored these variables from M^3s in the case
249 of African Suidae, where typically M^3 was the dominant molar for adults. However, this was
250 not necessary in the case of the Miocene suid species recorded at CLL1, where the scores for
251 M^2 and M^3 were the same. When the identification of a taxon was well-documented in the
252 literature and M^2s where available from CLL1, we focused on this material to score the FCT
253 variables. When any of these conditions did not apply, other dental (or even postcranial)
254 remains were studied to confirm or refine the taxonomic identifications. When no M^2s were
255 available from CLL1 for a particular taxon, FCT variables were based on those of the same
256 species or higher taxonomic ranks from elsewhere as reported in the literature.
257
258 *2.2. Ecometric analysis*
259 Functional crown types The FCT dental trait scoring scheme was designed to capture main
260 functional traits (durability, cutting, and other occlusal properties, as well as dental tissues) of
261 tooth shape and worn occlusal surfaces of herbivorous large mammal teeth, based on seven
262 (two ordinal and five binary) variables (Žliobaitė et al., 2016; Galbrun et al., 2018) that are
263 summarized in Table 3. The two ordinal variables, HYP and horizodonty (HOD; length of the
264 functional occlusal surface in terms of main cusp pairs) are related to tooth durability and have
265 three states each (Table 3). In turn, the binary variables record three additional functional
266 aspects, namely (Table 3): cutting structures (acute lophs [AL] and obtuse, or basin-like, lophs
267 [OL]); occlusion characteristics (structural fortification of cusps [SF] and occlusal topography
268 [OT]); and material properties (coronal cementum; CM). Based on data from extant
269 environments (national parks) from Kenya, these variables have been shown to be correlated
270 with environmental (climatic and ecological) parameters—such as precipitation (PREC),

temperature (TEMP), net primary productivity (NPP), and normalized difference vegetation index (NDVI; i.e., the greenness of the vegetation)—thus being promising for making paleoenvironmental inferences based on fossil data (Žliobaitė et al., 2016).

To retrodict the paleoenvironmental conditions of CLL1, we scored the seven FCT variables for the herbivorous large mammal species present at this locality and, based on the average for each variable, we followed the two different approaches described below. While FCT scoring scheme has remained fixed over the years, scoring conventions of selenodonts have changed from Oksanen et al. (2019) onward. For compatibility with the predictive models employed in our first approach, here we use the scoring conventions as they were defined in Žliobaitė et al. (2016), scoring all selenodonts with obtuse lophs and the Furchen of suids as fortified.

First approach Based on the seven FCT variables scored for 13 sites in Kenyan national parks, Žliobaitė et al. (2016) derived predictive models for 23 environmental (climatic and ecological) variables using least angle regression, which uses an iterative procedure to select the most informative dental trait predictors (while avoiding redundancies). The resulting regression models, to be used for predictive purposes, take the same functional form as ordinary linear regression (a linear combination of input variables). In our first approach, we used the 23 regression models (based on three FCT variables each) reported by Žliobaitė et al. (2016: Table 2; see our Supplementary Online Material [SOM] Table S1) to estimate 23 paleoenvironmental variables at CLL1. These regression models were not optimized for predictive purposes but rather for comparability of information content in different seasonality indices using a constant number of trait variables in each model. Yet, those models were tested for predictive accuracy at present day, and in principle can be used for analysis of the fossil record.

An obvious limitation of this approach is that the regression models are regional, calibrated on present day Kenya—no comparable models are available from elsewhere—which is not necessarily representative of past environments during the Iberian Miocene. On the other hand,

296 the geographically restricted nature of the dataset could also potentially result in a greater
297 optimization of the regression equations used to estimate the paleoenvironmental parameters.
298 In any event, we consider that the scope of the environments covered by the Kenyan localities
299 used to derived the models is compatible with a range of environments that can potentially be
300 expected at CLL1 and, thus, applicable to this fossil locality. Furthermore, precisely because of
301 the aformentioned limitation, we also followed an alternative approach that was not based on
302 such models but on the covariation between FCT variables and biomes in a much less
303 geographically restricted dataset.
304 Second approach As an alternative approach, we used principal component analysis (PCA) and
305 canonical variate analysis (CVA) performed with R v. 4.1.1 (R Core Team, 2021) through
306 Rstudio v. 2021.9.0.351 (Rstudio Team, 2021) to evaluate to what extent FCT variables
307 discriminate among different types of biomes and can be reliably used to make such inferences.
308 First, we used the Whittaker's system of present-day biomes to classify the 13 sites in Kenyan
309 national parks from Žliobaitė et al. (2016) based on their mean annual temperature (MAT) and
310 mean annual precipitation (MAP) into the different biomes of the world characterized according
311 to the distribution of vegetation types (Whittaker, 1975). We plotted them in the Whittaker
312 biomes diagram using the R packages 'devtools' v. 2.4.3 (Wickham et al., 2021), 'plotbiomes'
313 v. 0.0.0.9001 (Stefan and Levin, 2022) and 'ggplot2' v. 3.3.5 (Wickham, 2016), and performed
314 a PCA with not normalized input variables (i.e., the average values for each FCT variable at
315 each locality) using the R packages 'ade4' v. 1.7.18 (Chessel et al., 2004; Dray and Dufour,
316 2007; Dray et al., 2007; Bougeard and Dray, 2018; Thioulouse et al., 2018), 'factoextra' v. 1.0.7
317 (Kassambara and Mundt, 2020), and 'ggplot2' v. 3.3.5 (Wickham, 2016).
318 Second, we also relied on a geographically much wider dataset of FCT variables to further
319 asses if they are useful to correctly classify extant localities according to Whittaker biomes
320 using a CVA based on FCT data. In particular, we used Galbrun et al.'s (2018) dataset (available

online at https://github.com/zliobaite/teeth-redescription), which contains data from 28,886 localities around the world on environmental variables, species composition, and FCT variables for each species. We extracted the average of each FCT variable for those localities that, according to the Whittaker diagram, correspond to certain biomes that, based on previous literature (see Table 1), seem relevant to compare with CLL1 (temperate rainforest, temperate seasonal forest, tropical rainforest, tropical seasonal forest/savanna, and woodland/shrubland). The FCT variables mean hypsodonty and mean horizodonty were provided as three separate binary variables each in Galbrun et al.'s (2018) dataset but were transformed back to ordinal variables for this study. Once the localities were classified, we performed a cross-validated CVA on the same data, using biomes to distinguish a priori groups, with the R packages 'Morpho' v. 2.9 (Schlager, 2017) and 'ggplot2' v. 3.3.5 (Wickham, 2016). To better evaluate the structuration of the data and be able to discount spurious group separation, we computed the amount of variance (r^2) explained by group differences in the raw data and the CVA (with and without cross-validation) using a permutational multivariate analysis of variance (1000 permutations) with the R package 'RRPP' v. 1.3.1. (Collyer and Adams, 2018, 2019). Percentages of correct classification were computed based on the cross-validated CVA.

Finally, based on the CVA, CLL1 and the Kenyan localities were classified according to Whittaker's biomes. The probability that each locality belongs to one of the biomes distinguished a priori was evaluated based on the standard posterior probabilities of group membership (which add up to 1 when all the biomes distinguished a priori are considered) as well as the typicality probabilities (which test if a given locality falls outside the variation of each biome independently). To evaluate the consistency of the results for CLL1, the biome classification favored by the CVA posterior probabilities was compared with that obtained from the estimates of paleotemperature and paleoprecipitation yielded by the regressions based on FCT average values in our first approach. To further assess the reliability of the classification

346 provided by the CVA for CLL1, the classification for the nine Kenyan sites from Žliobaitė et
347 al. (2016) corresponding to the five relevant biomes included in the CVA was also compared
348 with that obtained from actual data on temperature and precipitation.
349
350 **3. Results**
351 Species identification An updated list of mammals from CLL1 is reported in Table 2. The
352 herbivorous large mammals included in FCT analyses include 20 species from 19 genera and
353 13 families, while the complete mammal list includes 78 species (39 small and 39 large
354 mammals). While a few small mammal species are added here, the number of large mammal
355 species from CLL1 (39) reported in Table 2 is lower than the figure of 47 species reported by
356 Alba et al. (2011a), and even the figure of 41 currently recognized by the NOW database (The
357 NOW Community, 2023). All these changes are not attributable to recovery of new taxa during
358 the new campaigns since 2010, but rather to the ongoing revision of the collections recovered
359 in previous decades.
360 With regard to micromammals, the most updated list of eulipotyphlans from CLL1 is
361 probably that reported by Van den Hoek Ostende and Furió (2005). The current list differs in
362 the following regards: (1) the galericine previously assigned to *Parasorex socialis* is attributed
363 to *Parasorex* sp., pending illumination of the relationship between *Parasorex ibericus* and the
364 central European '*Schizogalerix*' *voesendorfensis*; (2) the erinaceid previously attributed to
365 *Postpalerinaceus vireti* by Crusafont Pairó and Gibert Clols (1974) is considered to represent
366 a different species (tentatively referred to cf. *Postpalerinaceus* sp.); (3) besides *Talpa*
367 *vallesiensis*, two additional talpids (*Desmanella* sp. and *Talpa* sp.) are recorded; (4) the
368 heterosoricid present at the site is *Dinosorex grycivensis* instead of *Dinosorex sansaniensis* (see
369 Furió et al., 2015); (5) an additional dimylid (*Metacordylodon schlosseri*) and three additional
370 soricids (*Miosorex grivensis*, *Lartetium* sp., and *Paenelimnoecus* sp.) are identified. An

371 indeterminate chiropteran and a single lagomorph (contra Alba et al., 2011a) are also identified
372 at CLL1. As for the rodents, the list is taken from Casanovas-Vilar et al. (2016b), and only the
373 genus ascription of *Csakvaromys bredai* has been updated following Sinitsa et al. (2022).
374 Regarding the macromammals from CLL1 not included in the FCT computations, most
375 changes correspond to carnivorans. Their list is based on the review by Robles et al. (2014),
376 with several subsequent updates: (1) no material of *Promephitis pristinidens* has been
377 identified, and it is thus considered that previous citations of this genus from CLL1 correspond
378 to *Mesomephitis medius*; (2) *Hoplictis petteri* is considered a junior subjective synonym of
379 *Eomellivora fricki* following Valenciano et al. (2019); (3) a single hyaenid (*Protictitherium*
380 *crassum*) is recognized from CLL1; (4) the two amphicyonids from the site, currently under
381 study, are provisionally attributed to *Amphicyon* sp. and *Ammitocyon* sp.; (5) three ursids are
382 recorded, but instead of two *Ursavus* species, only *Ursavus brevirhinus* is present at the site,
383 with scarce dental material being attributable instead to *Miomaci* sp.—an indarctin ursid genus
384 present at Rudabánya and Can Poncic (de Bonis et al., 2017). In addition, the hyracoid is
385 assigned to *Pliohyrax rossignoli* following Pickford et al. (1997), although more detailed
386 comparisons of the scarce material available would be required to confirm such an attribution.
387 The remaining large mammals are those included in the FCT analyses and hence discussed in
388 greater detail in the following paragraphs, as they constitute the basic information needed to
389 replicate our results. An argument could be made that hyraxes should be included in the FCT
390 computations but we decided to exclude them as they were not considered in the equations
391 originally derived by Žliobaitė et al. (2016).
392 Two proboscidean species are recorded, a deinothere and a gomphothere. The deinotheriid
393 remains from CLL1 were described by Bergounioux and Crouzel (1962), who attributed them
394 to *Deinotherium giganteum*, which is currently considered the only deinotheriid species present
395 in MN9 of Europe (e.g., Pickford and Pourabrishami, 2013; Alba et al., 2020). The

396 gomphotheriid remains were described by Mazo (1977), who attributed them *Tetralophodon*
397 *longirostris*, which replaced *Gomphotherium angustidens* in late MN7+8 (Mazo and Van der
398 Made, 2012).

399 Perissodactyls are represented at CLL1 by six species (a chalicothere, a horse, three
400 rhinoceroses, and a tapir). The chalicotheriid remains are unpublished but were reported as
401 *Chalicotherium grande* (currently *Anisodon grande*) by Mein (1990) and later reassigned to
402 *Chalicotherium goldfussi* by Heissig (1999). The latter assignment is confirmed here based on
403 the position of the M^1 and M^2 metacones (see Anquetin et al., 2007), in further agreement with
404 the MN9 age of the site (the two species only overlap in late MN7+8; Anquetin et al., 2007).
405 The equid remains were attributed to *Hipparion primigenium primigenium* by Alberdi (1974).
406 Following Bernor et al. (1980, 1996, 2021), these remains could be assigned to a distinct species
407 endemic of the Vallès-Penedès Basin (*Hippotherium catalaunicum*). However, a long needed
408 revision of the Vallès-Penedès *Hippotherium* remains has been undertaken by some of the
409 authors of this paper and, on this basis, we prefer to tentatively assign the CLL1 remains to
410 *Hippotherium* cf. *primigenium*. This is because differences with the vast sample of this species
411 from Höwenegg (Bernor et al., 1997, 2022), at present time, do not seem to warrant a species
412 distinction. The rhinocerotid remains from CLL1, in turn, were described by Santafé Llopis
413 (1978), being attributed to four species, whose genus attribution has been updated based on
414 Sanisidro and Cantalapiedra (2022). Although these authors reported four species from CLL1,
415 we refrained from including *Lartetotherium sansaniense*, because it identification by Santafé
416 Llopis (1978) relies on a single damaged scaphoid that displays aceratheriine affinities. A
417 preliminary revision of the remains from the other rhinocerotid species by one of the authors of
418 this paper further indicates that more in-depth revision is required. On the one hand, the species
419 attribution of the *Dihoplus* remains must be considered tentative, because they show some
420 dental differences as compared with *Dihoplus schleiermacheri* from Central Europe. For the

same reason, the identification of *Aceratherium incisivum* is even more tentative and the remains might even belong to a different genus, as they display some dental features that fall outside the normal variation of the genus as recorded in Central Europe. Finally, the tapirid remains were described by Golpe-Posse and Crusafont-Pairó (1982), who attributed them to *Tapirus priscus*, an attribution that is confirmed here.

Artiodactyls are more diverse than perissodactyls, being represented at CLL1 by 11 species (four suids, a tragulid, a moschid, two bovids, two cervids, and a giraffid), although only the suid *Parachleuastochoerus crusafonti*, the bovid *Miotragocerus pannoniae*, and at least one of the cervids are common faunal elements. The suid remains were described by Golpe-Posse (1971, 1972), who recognized four different species: *Listriodon splendens*, *Pa. crusafonti*, *Hyotherium soemmeringi*, and ?*Hyotherium* sp. Pickford (1981, 2014) provided additional descriptions of the *Pa. crusafonti* sample from CLL1, which is the type locality of the species. The identification of *L. splendens* at CLL1 by Golpe-Posse (1971, 1972) was based on two teeth, a purported molar and a premolar, the latter being assigned by the same author to ?*Hyotherium* sp. The revision of the material indicates that the former belongs in fact to *T. priscus* and the latter to *Pa. crusafonti*. However, two infantile specimens reported by Van der Made (1996) and a few additional unpublished deciduous teeth confirm the presence of *L. splendens* at CLL1, representing the last well-dated occurrence of the genus in Europe (Van der Made et al., 2022). The larger-bodied tetraconodontine from CLL1 identified by Golpe-Posse (1971, 1972) as *Hy. soemmeringi* was later reassigned to *Conohyus steinheimensis* by Van der Made (1990). The species was later included in *Parachleuastochoerus steinheimensis* and, more recently, split into *Versoporcus steinheimensis* and *Versoporcus grivensis* by Pickford (2014, 2016). However, the revision of the single premolar attributed by Golpe-Posse (1971, 1972) to *Hy. soemmeringi* indicates that, together with an incisor, it belongs to the larger tetraconodontine referred by Pickford (2014, 2016) to *Parachleuastochoerus valentini* (see also

McKenzie et al., 2023). The presence of a suine at CLL1 was first reported by De Bruijn et al. (1992) as *Korynochoerus palaeochoerus* (currently *Propotamochoerus palaeochoerus*; e.g., Van der Made et al., 1999; McKenzie et al., 2023), apparently based on unpublished material not yet available to Golpe-Posse (1971, 1972). The revision of the suid remains from CLL1 unambiguously confirms the presence of the species based on diagnostic dentognathic material.

The tragulid remains from CLL1, originally reported as *Dorcatherium* sp. (Crusafont Pairó, 1958), were subsequently identified as *Dorcatherium naui* by Moyà-Solà (1979; see also Alba et al., 2011c). The material is scanty and consists of a few tarsal bones and an upper canine. The even scarcer moschid remains from CLL1 are unpublished. Based on their small size and some details of occlusal morphology, they are referred to *Micromeryx* aff. *flourensianus* but probably belong to an undescribed species. The bovid remains from CLL1 were described by Moyà-Solà (1983) as *Protragocerus* aff. *chantrei* and *Miotragocerus* aff. *pannoniae*, but we concur with previous authors (e.g., Alba et al., 2011a) that open nomenclature (aff.) is unnecessary for these attributions, which are not tentative. The cervid remains from CLL1 have not been described in detail but were assigned to *Amphiprox anocerus* by Azanza and Menéndez (1990). Our review of the abundant material available from CLL1 indicates that dental variation would be compatible with the presence of a single species. However, the variation displayed by the antler material strongly suggests the presence of a second species, the taxonomic identity of which cannot be clarified at the moment—although an assignment to *Euprox dicranoceros*, present in earlier Vallesian sites (Azanza and Menéndez, 1990), seems unlikely. The giraffid remains from CLL1 were described by Crusafont Pairó (1952), who assigned them to *Palaeotragus* sp. Here, however, they are merely referred to Giraffidae indet. because the available material merely consists of a few isolated postcranial elements that do not allow for a species or genus attribution, particularly taking into account the taxonomic uncertainties about the MN9 giraffids from the Vallès-Penedès Basin (Alba et al., 2022b).

Finally, as explained in greater detail in the Introduction, the hominid remains from CLL1 were first reported by Crusafont-Pairó (1958). The material currently available was described in detail by Begun et al. (1990), Golpe-Posse (1993), and Alba et al. (2012a). Although Crusafont Pairó and Hürzeler (1961, 1969) and subsequently Golpe-Posse (1993) recognized the presence of various species, currently the whole sample is attributed to *Hispanopithecus laietanus* (Alba, 2012; Alba et al., 2012a). Nevertheless, based on enamel–dentine shape, the presence of a second hominoid species at CLL1 cannot be entirely ruled out (Zanolli et al., 2023).

Paleoenvironmental estimates based on the first approach The values for the FCT variables for the investigated species recorded at CLL1 are reported in Table 4, while the 23 estimated environmental variables for this site are reported in Table 5. Most noteworthy are the estimated values of paleotemperature (MAT = 25 °C) and paleoprecipitation (MAP = 881 mm), which indicate a Whittaker's biome of tropical seasonal forest/savanna for CLL1 (Fig. 2).

Paleoenvironmental estimates based on the second approach The first two principal components of a PCA based on FCT variables for 13 extant localities from Kenyan national parks (Fig. 3) summarize more than 75% of the variance. The first principal component (56% of the variance) is mostly driven by SF and AL toward negative scores, and the remaining FCT variables toward positive scores. The site of CLL1 displays very high scores along this axis, most similar to the extant localities of Shimba Hills (tropical seasonal forest/savanna) as well as Elgon and Kakamega (temperate seasonal forests). Along PC1, these three extant localities fall far from the rest of extant localities, which cluster close to one another despite corresponding to the four different biomes included in the analysis. The second principal component (21% of the variance) is mostly driven by SF (and, to a lesser extent, CM and HYP) toward negative scores, and by AL (and, to a much lesser extent, OT and OL) toward positive scores. Extant Kenyan localities corresponding to the temperate seasonal forest and

woodland/shrubland biomes tend to display lower PC2 scores than those representing the tropical seasonal forest/savanna and subtropical desert biomes. The site of CLL1 displays an extremely positive score along this axis, well beyond any of the extant localities, suggesting relevant environmental differences even compared with the closest extant localities in PC1.

The CVA based on 18,671 extant localities from five different biomes accounts for 33.7% of the differences among the groups, which are statistically significant at $p < 0.001$, both with and without cross-validation. Differences among the groups are also statistically significant ($p < 0.001$) based on the raw data—indicating that grouping structure is not spurious—although they explain a lower amount of variance (13.9%). The cross-validated CVA has a low classification accuracy (49.5% after cross validation; Table 6) because there is a considerable overlap among several biomes (Fig. 4). The first canonical variate summarizes most of the variance (96%), being mostly determined by OL and, to a lesser extent, CM toward positive scores, and in decreasing order of importance, HOD, AL, and HYP toward negative scores. The analysis discriminates well between woodland/shrubland and tropical rainforest localities, and also quite well between the former and tropical seasonal forest/savanna localities (only with slight overlap of their 95% confidence ellipses). However, there is considerable overlap among these and other biomes, with the ellipse of the tropical rainforest biome being totally included within those of both the temperate rainforest and the tropical seasonal forest/savanna biomes, and further partly overlapping with that of the temperate seasonal forest biome. The second canonical variate is positively driven by most of the variables to some extent, except OL (which has no influence) and AL (which has a moderate influence toward negative scores). Given the small amount of variance summarized by CV2 (3.5%), it is questionable whether it needs to be interpreted, as further confirmed by the fact that all the five investigated biomes overlap along this axis. However, it is noteworthy that the tropical rainforest biome shows a lower range of variation than the remaining ones, with all the localities included displaying negative scores for

both CV1 and CV2. The locality of CLL1 also displays moderately negative scores for both axes, falling within the overlap zone among the ellipses of tropical seasonal forest/savanna, temperate rainforest, and tropical rainforest, and at the fringe of temperate seasonal forest.

However, based on the posterior probabilities (Table 7)—which hold assuming that the distribution of possible climatic conditions in the past is similar to that of the reference dataset of the present day—CLL1 is classified as a tropical rainforest as a first option (63%) and as a tropical seasonal forest/savanna as second option (30%). The typicality probabilities (Table 7) are consistent with such classifications and confirm that, based on FCT variables, CLL1 statistically differs from all the remaining biomes at least with $p < 0.05$. The second classification option for CLL1 (tropical seasonal forest/savanna) according to the CVA based on FCT variables coincides with the biome attribution of our first approach—i.e., based on estimated paleotemperature and paleoprecipitation using Žliobaitė et al.'s (2016) regressions. Estimates of paleotemperature and paleoprecipitation are based on different sets of variables (OL, SF, and OT vs. HOD, SF, and OT, respectively) than those that have greater loadings on CV1 (OL, HOD and, to a lesser extent, AL and HYP), so it is not surprising that the classification results yielded by these two different approaches do not completely match. However, it is remarkable that the second classification option obtained from the CVA, with a lower posterior probability (30%), does coincide with the biome classification obtained from paleotemperature and paleoprecipitation estimates based on FCT variables. The biome classification results for the extant Kenyan localities based on the CVA only coincide with those based on actual data of temperature and precipitation in five out of nine cases (Table 8), which is not surprising given the classification accuracy of the analysis around 50%. The mismatches correspond to localities from the temperate seasonal forest biome that are erroneously classified by the CVA as tropical seasonal forest/savanna, whereas the four localities actually corresponding to tropical seasonal forest/savanna are (like CLL1) correctly

546 classified as such. It must be taken into account, however, that none of the localities from
547 Kenyan national parks correspond to the tropical rainforest biome. The percentages of correctly
548 classified cases for the 18,671 localities included in the CVA (Table 6) indicate that localities
549 from the tropical seasonal forest/savanna biome are frequently erroneously classified as tropical
550 rainforest (indeed, which the same frequency as the former are correctly classified, 42%),
551 whereas tropical rainforest localities are most frequently correctly classified as such (82% of
552 the cases) and misclassified as tropical rainforest/savanna with a low frequency (9%).
553
554 **4. Discussion**
555 Environmental estimates and biome classification based on functional crown type variables The
556 23 prediction equations for environmental variables reported by Žliobaitė et al. (2016) vary in
557 both accuracy (r^2, measuring the goodness of fit) and predictive power (r^2*, as measured by
558 cross-validation). The former values vary from ~0.6–0.8 in the most reliable variables to less
559 than 0.3 in the least ones, resulting in highly divergent equations in terms of their potential
560 predictive power. While these models were not optimized to maximize the predictive accuracy,
561 the calibration accuracy is reasonable for trying them for predictive purposes on the fossil
562 record. Probably, more accurate equations could be derived in the future based on a higher
563 number of extant localities. In the meantime, the paleoenvironmental estimates derived from
564 these equations for CLL1 should be taken with care as rough approximations whose reliability
565 depends on the accuracy of the equations used to derive them. In other words, these estimates
566 should not be taken at face value, because the model calibration accuracy (or goodness of fit,
567 r^2) and, especially, the predictive power of these equations (calibration accuracy as measured
568 by cross-validation, r^{2*}) are quite low and there is no guarantee that the Kenyan extant localities
569 used to derive the models are representative of European environments during the Miocene.

570 Nevertheless, the estimated parameters could be useful in relative terms to compare CLL1 with
571 other well-sampled fossil localities of the Vallès-Penedès Basin in the future.
572 For the purposes of this work, estimates of paleotemperature (especially MAT) and
573 paleoprecipitation (MAP) will be mainly discussed here. Neither MAT nor MAP estimates
574 appear particularly accurate, with r^2 = 0.57 and 0.68, and r^2* = –0.05 and 0.38, respectively.
575 Based on the equations' accuracy, the paleoprecipitation estimate would be a priori more
576 reliable, but this is uncertain because Žliobaitė et al. (2016) provided no method for computing
577 the confidence intervals of such estimates. In any event, the biome classification based on the
578 paleotemperature (MAT) and paleoprecipitation (MAP) estimates for CLL1 should be
579 contrasted with other sources of evidence, such as those derived from stable isotope
580 composition of mammalian tooth enamel (e.g., Koch, 1998; Kohn et al., 1998; Domingo et al.,
581 2013; Higgins, 2018). These analyses are currently underway, but only preliminary results have
582 been published so far (see below for further details). In the meantime, an alternative approach
583 based on a multivariate analysis of FCT average values was undertaken to contrast the biome
584 classification for CLL1 with that discussed above based on the regression equations.
585 Based on the estimated values for paleotemperature (25 °C) and paleoprecipitation (881
586 mm), CLL1 would correspond to a tropical seasonal forest/savanna according to Whittaker's
587 biome scheme. The biome classification based on the CVA is not entirely coincident, as CLL1
588 is classified as a tropical rainforest with a posterior probability of 63%. Such a discrepancy is
589 not surprising, as the CVA is based on the seven FCT variables, whereas the paleotemperature
590 and paleoprecipitation estimates are calculated from different subsets of three variables each,
591 overall including only four out of the seven FCT variables. Furthermore, the classification
592 accuracy of the CVA is moderately low (49.5%). Given all these caveats, it is remarkable that
593 the biome classification based on paleoenvironmental estimates (tropical seasonal
594 forest/savanna) coincides with the second most likely classification of the CVA, with a

posterior probability of 30%. From a purely statistical viewpoint, CLL1 falls in an area of the ecomorphospace where the 95% confidence ellipses of both biomes overlap, with the tropical rainforest biome displaying a much more restricted scatter than tropical seasonal forest/savanna. Moreover, extant localities from the tropical seasonal forest/savanna biome are as frequently misclassified as tropical rainforest as correctly classified (42% in both cases), whereas tropical rainforest localities are most frequently classified correctly and only seldom misclassified as tropical seasonal forest/savanna. Therefore, it seems logical to conclude that CLL1 most likely belongs to the tropical seasonal forest/savanna biome. Alternatively, CLL1 might belong to a tropical rainforest biome, which differs from the tropical seasonal forest/savanna biome by displaying much higher precipitation values. This would imply that the annual precipitation estimate derived for CLL1 largely underestimates the actual value, which must be more than twice the estimate (>2500 mm instead of 881 mm at 25 °C, based on Whittaker's scheme). This seems unlikely even if paleotemperature is overestimated, but not completely impossible, given the low accuracy of the paleoprecipitation regression equation. A third possible explanation, not mutually exclusive with the first one, is that CLL1 records a mosaic of habitats that, despite falling within the tropical seasonal forest/savanna biome, mimics the faunal composition that would be expected in a tropical rainforest habitat—owing to local paleoenvironmental conditions favoring the presence of taxa adapted to more humid environments. These possibilities are evaluated in the next subsection based on the fossil flora and fauna from CLL1, as well as in relation to preliminary data on tooth enamel isotopic data.

Whittaker's biome classification is one of the simplest schemes to distinguish terrestrial biomes as it only considers MAT and MAP. While the scheme is calibrated on the present day and, in all probability, does not identically apply to the deep past, it can be applied to the Miocene to a first approximation. Other biome classification systems, such as Walter (1979), consider seasonality in both temperature and precipitation. Since the methods used allow

620 inferring which are the coldest/warmest and wettest/driest months in the studied localities these
621 biome classification schemes can be considered as well. MAT is above 20 °C, which indicates
622 a tropical climate (according to Köppen-Geiger climate classification; see Peel et al., 2007)
623 with little temperature seasonality since it ranges from 24.4 °C in the coldest month to 26.7 °C
624 in the warmest. MAP is also high (881 mm) for a tropical environment such as savanna or desert
625 with average monthly precipitation always above 100 mm. However, inferred rainfall
626 seasonality is remarkable, with precipitation in the wettest month (2119 mm) being more than
627 10 times higher than that recorded during the driest month (136 mm). Such precipitation
628 seasonality is consistent with a tropical seasonal biome, with a clear rainy season. Nonetheless,
629 there is a gradient between evergreen tropical forests and tropical deciduous forests depending
630 on the length and severity of the dry season, with tropical seasonal forests (also called
631 semievergreen or mixed tropical forests), corresponding to zonoecotone I/II of Walter (1979),
632 showing an intermediate composition, characterized by the presence of some deciduous tree
633 species that lose their leaves during the dry season. Vegetation structure in tropical seasonal
634 forests includes different canopy layers as in rainforests, but generally stratification is less
635 complex, the canopy is relatively more open, epiphytes and especially lianas are abundant, and
636 ground vegetation is more diverse and abundant (see Walter, 1979; Allaby, 2006). In a tropical
637 seasonal biome, the driest month typically records less than 60 mm of rainfall, which is much
638 lower than the values inferred for CLL1, suggesting that the latter might have been
639 characterized by a tropical seasonal forest somewhat intermediate between a tropical evergreen
640 and a tropical deciduous forest.
641 Comparison with previous paleoenvironmental inferences for Can Llobateres 1 The summary
642 of previous paleoenvironmental inferences for CLL1 provided in Table 1 highlights some
643 similar conclusions among authors but also some discrepancies regarding the openness of the
644 habitat and the seasonality of the climate. Nagatoshi (1987) concluded that most of the primate-

bearing sites of the Middle and Late Miocene of western Eurasia were characterized by the presence of water and interpreted CLL1 as an open environment with some intruding marshy areas based on the presence of *Hippotherium* and *Tapirus*. However, the paleobotanical evidence is rather suggestive of a closed forest next to a marshy area with more open environments at some distance (Fig. 5; Marmi et al., 2012). The fossil plant assemblage from CLL1 (Álvarez Ramis, 1975; Sanz de Siria Catalán, 1993, 1994; Marmi et al., 2012) is composed of abundant reed remains (*Phragmites* and *Typha*), coupled with palms, evergreen laurels, and fig trees (*Ficus* sp.). The reeds are suggestive of a marshy area, whereas the rest of the vegetation denotes the nearby presence of a dense wetland or riparian forest (Alba et al., 2011a, 2011b; Marmi et al, 2012; Andrews, 2015). In turn, the presence of mega-mesothermal taxa and the absence of deciduous taxa indicate a subtropical to warm-temperate climate characterized by high mean annual temperatures (Marmi et al., 2012). Sanz de Siria Catalán (1994) inferred subtropical conditions based on the then available flora from CLL1. Although such inferences must be taken with care, given that CLL1 corresponds to an azonal plant community, they are consistent with the estimated MAT of 26 °C derived in this work from FCT variables. According to the Köppen-Geiger climate classification (updated by Peel et al., 2007), a tropical climate is characterized by average temperatures above 18 °C in the coldest month, whereas a subtropical (or temperate) climate displays average temperatures above 10 °C in the hottest month and between 0 and 18 °C in the coldest month. Therefore, the paleotemperature estimates for CLL1 based on FCT variables for the hottest month (26.7 °C) and the coldest month (24.4 °C) indicate a tropical climate, consistent with the two biome attributions favored by the analyses. On the other hand, paleobotanical evidence from other localities and nearby basins suggests that the plant community from CLL1 would not be representative of the zonal vegetation, which would have been characterized by a higher proportion of mega-mesothermal taxa and deciduous elements, overall denoting subtropical to

warm-temperate (rather than tropical) climate conditions in the Vallès-Penedès Basin around the transition between the early and late Vallesian (Marmi et al., 2012, and references therein). It is thus reasonable to assume that, far from the wetlands, more open woodlands would have been present by this time (Alba et al., 2011a, 2011b; Marmi et al., 2012), and that paleotemperature estimates for CLL1 based on FCT variables might be biased to some extent toward higher temperatures than were actually present in the area by that time.

As stressed by Marmi et al. (2012) and Andrews (2015), the faunal composition of CLL1 further supports the presence of a marshy depositional environment, given the presence of beavers and otters (Marmi et al., 2012; Andrews, 2015), the bovid *M. pannoniae* (which displays adaptations to wet environments; Köhler, 1993), and the tragulid *D. naui* (which shows many similarities with the extant water chevrotian, a forest-dwelling frugivorous animal with aquaphilous preferences; Alba et al., 2011c, and references therein). The presence of large browsing herbivores (*C. goldfussi*, *M.* aff. *flourensianus*, *A. anocerus*, *T. priscus*, *Ac. incisivum*, and *Alicornops simorrense*), in turn, is indicative of a densely forested environment (Marmi et al., 2012), which is further supported by a diverse assemblage of flying squirrels and tree dormice, which are quite diverse albeit not particularly abundant (Casanovas-Vilar and Agustí, 2007; Marmi et al., 2012; Casanovas-Vilar et al., 2015). Flying squirrels are remarkably diverse, including up to five different species representing both large (*Miopetaurista crusafonti*, *Miopetaurista neogrivensis*, *Albanensia* aff. *grimmi*) and small (*Blackia miocaenica*., cf. *Pliopetaurista* sp.) species. Such diversity of flying squirrels is currently only recorded in the tropical and subtropical forests of southeastern Asia, which show a complex and stratified canopy (Jackson 2012, Lu et al. 2013). This is further consistent with the presence of a large-bodied ape such as *H. laietanus*, particularly given the previous locomotor inferences based on its partial skeleton, indicating that it possessed an orthograde body plan with suspensory adaptations, even if displaying a higher degree of above-branch quadrupedalism than extant

apes (Moyà-Solà and Köhler, 1996; Almécija et al., 2007; Alba et al., 2010, 2012b; Pina et al., 2012; Tallman et al., 2013; Susanna et al., 2014). On the other hand, the presence of a giraffid (Köhler, 1993) and rodents such as the cricetid *Hispanomys* and ground squirrels (Casanovas-Vilar and Agustí, 2007) hint at the presence of more open woodlands nearby (Marmi et al., 2012).

Unlike other artiodactyls, suids have not been previously considered when making paleonvironmental inferences for CLL1, even though they can provide interesting insights. The taxonomic revision of the large herbivorous mammals from CLL1 performed in this work has confirmed the presence of a diverse suid assemblage, clearly dominated by the small tetraconodontine *Pa. crusafonti*, but further including (in order of decreasing abundance) *P. palaeochoerus*, *L. splendens*, and *Pa. valentini*. The dietary ecology of *L. splendens* has been thoroughly discussed, as these suids stand out by its lophodont morphology and the lack of adaptations for the rooting feeding behaviors characteristic of most suids (Fortelius et al., 1996a; Van der Made et al., 2014, 2022), allowing them to survive when other types of food are scarce. The occlusal morphology of *L. splendens* was originally interpreted as an adaptation for a mainly folivorous diet (Van der Made, 1996) and microwear analyses supported that this species was mainly a browser (Hunter and Fortelius, 1994). This has been confirmed by isotopic analyses, which further suggest a considerable consumption of fruits and maybe some grass (Aiglstorfer et al., 2014). Van der Made et al. (2014) hypothesized that *L. splendens* would have inhabited relatively open or mosaic environments, but most recently Van der Made et al. (2022) favored the view that, given the lack of rooting adaptations, *Listriodon* would have been more limited than other suids to environments where nutritious leaves and fruits were available throughout the year. Based on dental morphology, it has been inferred that *P. palaeochoerus* would have been even better adapted for rooting behaviors than medium to large-sized tetraconodontines of the genera *Parachleuastochoerus* and *Versoporcus* (Van der Made, 2010;

720 Van der Made et al., 2014). However, isotopic data indicate that these tetraconodontines also
721 consumed underground resources (Aiglstorfer et al., 2014), and indeed isotopic data and trace
722 elements from Rudabánya (Hungary)—a hominoid-bearing site roughly coeval to CLL1—
723 indicate that tetraconodontines might have feed on such resources more frequently than
724 *Propotamochoerus* (Eastham et al., 2016, 2017; Iannucci and Begun, 2022). This suggests a
725 more varied omnivorous diet for *Propotamochoerus*, in agreement with the greater
726 development of secondary cusps typical of suines (Fortelius et al., 1996a).

727 These dietary inferences for suids recorded at CLL1 are relevant for interpreting the
728 extinction of *H. laietanus* because some parallelism can be established with the diet of *H.*
729 *laietanus* and also because the extinction of *L. splendens* has been related to the
730 paleoenvironmental changes during the early/late Vallesian transition, which are generally
731 considered the trigger of the Vallesian Crisis (Van der Made et al., 2022). The latter is a regional
732 turnover event, originally identified in the Vallès-Penedès Basin, that allegedly implied the
733 extinction of mammals adapted to warm and humid forested environments and their
734 replacement by taxa adapted to more open and drier environments (Agustí and Moyà-Solà,
735 1990; Moyà-Solà and Agustí, 1990). The extension of the Vallesian Crisis to a continental scale
736 (e.g., Fortelius et al., 1996b; Agustí et al., 1999) has been questioned (Casanovas-Vilar et al.,
737 2005, 2010), being alternatively attributable to sampling biases (Casanovas-Vilar et al., 2014,
738 2016a). This has been conclusively shown based on micromammals from the Vallès-Penedès
739 Basin (Casanovas-Vilar et al., 2014), where the correction of such biases indicates that the
740 purported Vallesian Crisis was a protracted faunal turnover rather than an abrupt extinction
741 event. Although this remains to be ascertained for large mammals, it has been convincingly
742 argued that changes in vegetation structure led to the extinction of multiple forest-adapted
743 frugivorous taxa, particularly primates (Agustí et al., 2003; Marmi et al., 2012; Casanovas-
744 Vilar et al., 2016a) and some suids (Van der Made et al., 2022).

745 Dental microwear analyses indicate that *H. laietanus* displayed a frugivorous diet (Ungar,
746 1996; DeMiguel et al., 2014), probably emphasizing soft ripe fruits but also including hard
747 fruits as fallback fruits on a seasonal basis (DeMiguel et al., 2014). This would have allowed
748 this species to survive in the face of marked environmental instability around the early/late
749 Vallesian transition. This is supported by the presence of abundant enamel hypoplasias (Skinner
750 et al., 1995; Eastham et al., 2009), which indicate repeated episodes of malnutrition due to
751 seasonal resource abundance fluctuations, suggesting that *H. laietanus* probably feed on hard
752 foods during the unfavorable season (DeMiguel et al., 2014). Although there are no
753 paleodietary data for *Pa. crusafonti*, small suids are generally interpreted as forest-adapted
754 forms (Fortelius et al., 1996a), in agreement with the abundance in this taxon at CLL1. This
755 suggests that *Pa. crusafonti* might have displayed on the ground a similar feeding strategy to
756 that of *H. laietanus* in an arboreal niche, i.e., predominantly based on fruits and recoursing to
757 other resources during the most unfavorable months of the year (maybe thanks to rooting
758 behaviors). The moderately abundant *P. palaeochoerus*, like the scarce *Pa. valentini*, could
759 have exploited other trophic resources and preferentially inhabited the more open areas far from
760 the wetland. In contrast, this explanation is more unclear in the case of *L. splendens*, whose
761 scarcity at CLL1 might be related to the lack of a continuous fruit supply during the unfavorable
762 season, given its lack of rooting adaptations.
763 With regard to the biome classification of CLL1 as a tropical rainforest or a tropical seasonal
764 forest/savanna biome, it is worth comparing it with the results obtained by previous authors
765 using different methods. The analyses of mammalian community structure performed by
766 Andrews (1996) using different methods reconstructed both CLL1 and Rudabánya as
767 subtropical seasonal forests, thus supporting a classification of the former as a tropical seasonal
768 forest rather than as a tropical rainforest (note that an alternate classification of CLL1 as a
769 temperate rain or seasonal forest biome is discounted by the results of our analyses). Similarly,

based on multivariate analyses of faunal composition, Hernández Fernández et al. (2003) classified CLL1 as a deciduous tropical forest with a posterior probability of 99.5%—the second option (savanna) and other remaining possibilities (rainforest and laurel forest) being very small. Despite being based on a much less sophisticated approach, the results of Hernández Fernández et al. (2003) are also broadly consistent with those derived in this work, supporting that CLL1 is more readily interpreted as a tropical seasonal forest/savanna biome than as a tropical rainforest. By contrast, Costeur's (2005) cenogram analyses concluded that CLL1 displayed more closed and humid conditions than Rudabánya, attributing the former to a tropical forest and the latter to a subtropical forest/savanna mosaic. Additional support to the classification of CLL1 as a tropical seasonal forest/savanna instead of a tropical rainforest comes from preliminary isotope analyses performed on muroid rodents from the Vallès-Penedès Basin (Casanovas-Vilar et al., 2019, 2020). These confirm that hominoid-bearing sites are more humid on average than those where primates are not recorded, with most of the former being in the range of tropical deciduous forests to evergreen warm mixed forests. For CLL1, paleoprecipitation estimates derived from muroid stable isotopes result in MAP well above 1000 mm while paleotemperature estimate is comparable to that derived in this work (I.C.V., unpublished data). Nevertheless, the value derived from isotopes is much lower than the one that would be expected for a tropical rainforest, confirming that CLL1 does not correspond to this type of biome. Unpublished isotope analyses based on the equid *Hip. catalaunicum* from CLL1 indicate a diet entirely based on C_3 vegetation (Misas Alcàntara, 2022). Following the methods by Kohn (2010), these can be used to infer paleoprecipitation, although ideally a broader taxonomic sample should be considered for the calculations. Tooth enamel $\delta^{13}C$ ranges from -10.7‰ to -12.5‰ (Misas Alcàntara, 2022), which results in a MAP estimation of ~700–1000 mm, thus consistent with the results yielded by the multivariate analyses of FCT variables. Misas Alcàntara (2022) noted that, if *Hip. catalaunicum* had inhabited and fed in the locally

795 humid environment next to the depositional environment, this would have resulted in more
796 negative isotopic values—in further agreement with the greater abundance of *Hippotherium*
797 remains in the channel deposits than in the primate-bearing levels of CLL1. Therefore, the
798 values reported are taken as an indication of less humid, and presumably more open,
799 environments nearby.

800 It has been hypothesized that *H. laietanus* would have preferred the humid forested
801 environments close to permanent water due to the availability of ripe, soft fruit supplies on a
802 year-round basis (Alba et al., 2011a, 2011b; Marmi et al., 2012), or at least during part of the
803 year (DeMiguel et al., 2014), despite the fact that warm-temperate mixed forests, composed
804 mainly of deciduous taxa, would have probably been present far from these wetlands (Alba et
805 al., 2011a, 2011b; Marmi et al., 2012). Similarly, the roughly coeval *Rudapithecus hungaricus*
806 from Rudabánya (Hungary) is associated with a subtropical swamp forest dominated by swamp
807 cypress (*Taxodium*; Andrews and Cameron, 2010; Andrews, 2015). Tooth enamel stable
808 isotope analyses of the large mammal assemblage of Rudabánya indicate a mosaic of
809 environments and ecological niche partitioning (Eastham et al., 2016). Some taxa, such as *D.*
810 *naui* and *C. goldfussi*, would have fed in closed canopy environments, while others such as
811 *Hippotherium intrans* would have preferred more open habitats. Therefore, the environment
812 associated with *R. hungaricus* in Rudábanyá has strong similarities with that associated with *H.*
813 *laietanus* in CLL1, the two corresponding to local wetlands. However, there are also some
814 differences because the riparian forest composition (as evidenced from paleobotanical data) is
815 clearly different and woodlands away from the wetlands appear to have been more humid and
816 warm-temperate in Rudabánya (Andrews, 2015).

817 Within such environments, Late Miocene dryopithecines occupied a mainly arboreal and
818 frugivorous niche. Although these environments might have been quite common in the Vallès-
819 Penedès Basin during the early Vallesian (Alba et al., 2011b; Marmi et al., 2012), from the late

Vallesian onwards, tropical and subtropical taxa (such as palm and fig trees) would have progressively disappeared as temperatures dropped (Sanz de Siria Catalán, 1994), while deciduous trees (such as poplars or willows) became dominant in forested areas and wetlands (Agustí et al., 2003; Alba et al., 2011a, 2011b; Marmi et al., 2012). As a result, these new environments would not have provided the necessary resources to sustain a population of *H. laietanus* (and other taxa dependent on forest trophic resources, such as probably *Pa. crusafonti* and *L. splendens*) throughout the year, especially during the cold season, leading to their progressive demise and eventual extinction in the Vallès-Penedès Basin and other areas of Western Europe (Agustí et al., 2003; Casanovas-Vilar et al., 2005, 2010; Alba et al., 2011a, 2011b; Marmi et al., 2012). In this regard, it is noteworthy that the record of *L. splendens* from CLL1 represents the latest well-dated occurrence of this taxon in Europe, whereas *Pa. crusafonti* is last recorded slightly later at La Tarumba 1 (Van der Made, 1990, 1997; Van der Made et al., 2022) at ~9.6 Ma (Casanovas-Vilar et al., 2016b), coinciding with the last record of *H. laietanus* (Casanovas-Vilar et al., 2011; Alba et al., 2018). The extinction of hominoids in other areas of Western mainland Europe would have followed a similar, although diachronous, pattern (Agustí et al., 2003; Casanovas-Vilar et al, 2010, 2011; Merceron et al., 2010; DeMiguel et al., 2014).

5. Conclusions

This study for the first time applied a full FCT scheme to analyze a Miocene fossil site. The results of this work indicate that FCT variables in combination with regional predictive models calibrated on Kenyan national parks as well as case-based reasoning over a selection of present-day biomes are not very powerful for providing unambiguous biome classifications for CLL1. Paleoprecipitation values appear potentially more biased than paleotemperature estimates, which show a greater agreement with isotopic data and both plant and faunal composition.

845 Canonical variate analyses, in turn, failed to distinguish some particular biomes. Nevertheless,
846 when both approaches based on FCT variables are combined, the results are in broad agreement
847 with previous inferences based on other sources of data, suggesting that FCT variables are a
848 useful complementary approach to make ecometric comparisons among multiple sites with
849 limited associated cost, thus being potentially useful to refine inferences based on other, more
850 traditional methods of paleoecological inference.

851 Regarding CLL1, the multivariate analyses based on FCT support a biome classification as
852 tropical rainforest or tropical seasonal forest/savanna, but paleotemperature and
853 paleoprecipitation estimates, particularly considering the amplitude of rainfall seasonality, are
854 in better agreement with the latter. These results are in further accordance with previous
855 inferences derived from fossil plants and mammals, as well as preliminary isotopic data. Based
856 on these other sources of evidence, it is concluded that the inability of the multivariate analysis
857 to unambiguously classify CLL1 as a tropical seasonal forest is due to the fact that the fossil
858 assemblage mixes forest-adapted taxa (such as *H. laietanus* and *Pa. crusafonti*), likely restricted
859 to the closed forest environment surrounding the marshy depositional area, with other taxa that
860 likely inhabited more open woodland environments far from the wetland (such as
861 *Propotamochoerus* and *Hippotherium*). In other words, the CLL1 local paleoenvironment to
862 which *H. laietanus* was adapted, in isolation, would not be representative of the biome at a
863 more regional scale, characterized by a mosaic of dense forests around the wetlands and more
864 open vegetation between these areas. Overall, our results are consistent with previous studies
865 that related the extinction of frugivorous hominoids in Western mainland Europe with that of
866 other forest-adapted taxa—the so-called Vallesian Crisis. Even though paleobiodiversity
867 analyses of micromammals suggest that this was a more protracted event rather than an abrupt
868 crisis, it remains to be determined if the same applies to large mammals or whether some
869 important paleoenvironmental threshold (such as the complete replacement of tropical seasonal

forest patches by deciduous tropical forests) was surpassed at ~9.5 Ma, at least in the Vallès-Penedès Basin. Future studies based on FCT variables in other well-sampled Vallesian localities of this basin, preceding (e.g., Castell de Barberà, Creu de Conill, Can Poncic) or postdating (e.g., La Tarumba, Torrent de Febulines) CLL1, might provide further precision in assessing the causes of the extinction of Miocene apes in Europe.

Acknowledgments

This article is part of R+D+I projects PID2020-117289GB-I00 and and PID2020-116220GB-I00, funded by the Agencia Estatal de Investigación of the Spanish Ministerio de Ciencia e Innovación (MCIN/AEI/10.13039/501100011033/), and has also been supported by the Agència de Gestió d'Ajuts Universitaris i de Recerca of the Generalitat de Catalunya (2001 SGR 00620) and the Generalitat de Catalunya/CERCA Programme, and the Government of Aragón (Research Group ref. E33_23R). S.G.A. enjoys a technician contract of the INVESTIGO Program 2022 (reference 100027TC1) financed by the European Union, Next Generation EU. I.Ž. acknowledges research funding by the Academy of Finland (grant no. 341623). O.C. gratefully acknowledges funding to R.L.B. (NSF ABI 1759882) and Howard University, for his support as a postdoctoral research fellow at Howard University, Washington D.C. We are grateful to Alessandro Urciuoli, Florian Bouchet, and Oriol Monclús-Gonzalo for statistical advice, as well as Salvador Moyà-Solà and Víctor Vinuesa for discussion about fossil material. This work is part of the Ph.D. Dissertation of the first author, in the framework of the Ph.D. Programme in Biodiversity of the Universitat Autònoma de Barcelona. Finally, we thank the Editor (Clément Zanolli), the Associate Editor, and three anonymous reviewers for helpful and constructive comments that helped us improve a previous draft of this paper.

References

895 Agustí, J., Moyà-Solà, S., 1990. Mammal extinctions in the Vallesian (Upper Miocene). Lect.
896 Not. Earth Sci. 30, 425–432.
897 Agustí, J., Köhler, M., Moyà-Solà, S., Cabrera, L., Garcés, M., Parés, J.M., 1996. Can
898 Llobateres: the pattern and timing of the Vallesian hominoid radiation. J. Hum. Evol. 31,
899 143–155.
900 Agustí, J., Cabrera, L., Garcés, M., Parés, J.M., 1997. The Vallesian mammal succession in the
901 Vallès-Penedès basin (northeast Spain): Paleomagnetic calibration and correlation with
902 global events. Palaeogeogr. Palaeoclimatol. Palaeoecol. 133, 149–180.
903 Agustí, J., Cabrera, L., Garcés, M., Llenas, M., 1999. Mammal turnover and global climate
904 change in the late Miocene terrestrial record of the Vallès-Penedès basin (NE Spain). In:
905 Agusti, J., Rook, L., Andrews, P. (Eds.), The Evolution of Neogene Terrestrial Ecosystems
906 in Europe. Cambridge University Press, Cambridge, pp. 397–411.
907 Agustí, J., Sanz de Siria Catalán, A., Garcés, M., 2003. Explaining the end of the hominoid
908 experiment in Europe. J. Hum. Evol. 45, 145–153.
909 Aiglstorfer, M., Bocherens, H., Böhme, M., 2014. Large mammal ecology in the late Middle
910 Miocene Gratkorn locality (Austria). Palaeobiodivers. Palaeoenviron. 94, 189–213.
911 Alba, D.M., 2012. Fossil apes from the Vallès-Penedès Basin. Evol. Anthropol. 21, 254–269.
912 Alba, D.M., Casanovas-Vilar, I., Moyà-Solà, S., Robles, J.M., 2011a. Parada 4. El Vallesiense
913 Inferior y su transición con el Vallesiense Superior: Can Llobateres. Paleontol. Evol.
914 memòria especial 6, 111–123.
915 Alba, D.M., Casanovas-Vilar, I., Robles, J.M., Marmi, J., Moyà-Solà, S., 2011b. New
916 paleontological excavations at the Late Miocene site of Can Llobateres 1 (Vallès-Penedès
917 Basin, NE Iberian Peninsula): preliminary results of the 2010 campaign. In: Pérez-García,
918 A., Gascó, F., Gasulla, J.M., Escaso, F. (Eds.), Viajando a Mundos Pretéritos. Ayuntamiento
919 de Morella, Morella, pp. 35–43.

Alba, D.M., Moyà-Solà, S., Robles, J.M., Casanovas-Vilar, I., Rotgers, C., Carmona, R., Galindo, J., 2011c. Middle Miocene tragulid remains from Abocador de Can Mata: the earliest record of *Dorcatherium naui* from Western Europe. Geobios 44, 135–150.

Alba, D.M., Casanovas-Vilar, I., Almécija, S., Robles, J.M., Arias-Martorell, J., Moyà-Solà, S., 2012a. New dental remains of *Hispanopithecus laietanus* (Primates: Hominidae) from Can Llobateres 1 and the taxonomy of Late Miocene hominoids from the Vallès-Penedès Basin (NE Iberian Peninsula). J. Hum. Evol. 63, 231–246.

Alba, D.M., Almécija, S., Casanovas-Vilar, I., Méndez, J.M., Moyà-Solà, S., 2012b. A partial skeleton of the fossil great ape *Hispanopithecus laietanus* from Can Feu and the mosaic evolution of crown-hominoid positional behaviors. PLoS One 7, e39617.

Alba, D.M., Casanovas-Vilar, I., Furió, M., García-Paredes, I., Angelone, C., Jovells-Vaqué, S., Luján, À. H., Almécija, S., Moyà-Solà, S., 2018. Can Pallars i Llobateres: A new hominoid-bearing locality from the late Miocene of the Vallès-Penedès Basin (NE Iberian Peninsula). J. Hum. Evol. 121, 193–203.

Alba, D.M., Gasamans, N., Pons-Monjo, G., Luján, À.H., Robles, J.M., Obradó, P., Casanovas-Vilar, I., 2020. Oldest *Deinotherium proavum* from Europe. J. Vertebr. Paleontol. 40, e1775624.

Alba, D.M., Torres, J., DeMiguel, D., Casanovas-Vilar, I., 2022a. The Vallès-Penedès Miocene Vertebrates Paleobiodiversity Database. In: Casanovas-Vilar, I., Alba, D.M. (Eds.), NOW 25th Anniversary Meeting. Sabadell (Barcelona), 16–18 November 2022. Abstract book & fieldtrip guide. Paleontol. Evol. memòria especial 9, 59–60.

Alba, D.M., Robles, J.M., Casanovas-Vilar, I., Beamud, E., Bernor, R.L., Cirilli, O., DeMiguel, D., Galindo, J., Llopart, I., Pons-Monjo, G., Sánchez, I.M., Vinuesa, V., Garcés, M., 2022b. A revised (earliest Vallesian) age for the hominoid-bearing locality of Can Mata 1 based on

new magnetostratigraphic and biostratigraphic data from Abocador de Can Mata (Vallès-Penedès Basin, NE Iberian Peninsula). J. Hum. Evol. 170, 103237.

Alberdi, M.T., 1974. El género *Hipparion* en España. Nuevas formas de Castilla y Andalucía, revisión e historia evolutiva. In: Trabajos sobre Neógeno-Cuaternario 1. Instituto Lucas Mallada, C.S.I.C., Madrid., pp. 1–219.

Allaby, M., 2006. Biomes of the Earth: Tropical forests. Chelsea House Publishers, New York.

Almécija, S., Alba, D.M., Moyà-Solà, S., Köhler, M., 2007. Orang-like manual adaptations in the fossil hominoid *Hispanopithecus laietanus*: first steps towards great ape suspensory behaviours. Proc. R. Soc. B. 274, 2375–2384.

Almécija, S., Hammond, A.S., Thompson, N.E., Pugh, K.D., Moyà-Solà, S., Alba, D.M., 2021. Fossil apes and human evolution. Science 372, eabb4363.

Álvarez Ramis, C., 1975. Quelques considérations écologiques sur le gisement Vallésien de Can Llobateres (Barcelone, Espagne). In: Comptes Rendus du 100e Congrès National des Sociétés Savantes (Paris, 1975). Fascicule II. Bibliothèque Nationale, Paris, pp. 11–16.

Andrews, P., 1996. Palaeoecology and hominoid palaeoenvironments. Biol. Rev. 71, 257–300.

Andrews, P., 2015. An Ape's View of Human Evolution. Cambridge University Press, Cambridge.

Andrews, P., Cameron, D., 2010. Rudabànya: Taphonomic analysis of a fossil hominid site from Hungary. Palaeogeogr. Palaeoclimatol. Palaeoecol. 297, 311–329.

Anquetin, J., Antoine, P.O., Tassy, P., 2007. Middle Miocene Chalicotheriinae (Mammalia, Perissodactyla) from France, with a discussion on chalicotheriine phylogeny. Zool. J. Linn. Soc. 151, 577–508.

Azanza, B., Menéndez, E., 1990. Los ciervos fósiles del neógeno español. Paleontol. Evol. 23, 75–82.

968 Begun, D.R., 1994. Relations among the great apes and humans: new interpretations based on
969 the fossil great ape *Dryopithecus*. Yearb. of Phys. Anthropol. 19, 11–63.
970 Begun, D.R., 2009. Dryopithecins, Darwin, de Bonis, and the European origin of the African
971 apes and human clade. Geodiversitas, 31, 789–816.
972 Begun, D.R., Moyá-Sola, S., Kohler, M., 1990. New Miocene hominoid specimens from Can
973 Llobateres (Vallès Penedès, Spain) and their geological and paleoecological context. J. Hum.
974 Evol. 19, 255–268.
975 Bergounioux, F.M., Crouzel, F., 1962. Les Deinothéridés d'Espagne. Bull. Soc. Geol. Fr. 4,
976 394–404.
977 Bernor, R.L., Woodburne, M.O., Van Couvering, J.A., 1980. A contribution to the chronology
978 of some Old World Miocene faunas based on hipparionine horses. Geobios 13, 705–739.
979 Bernor, R.L., Koufos, G.D., Woodburne, M.O., Fortelius, M., 1996. The evolutionary history
980 and biochronology of European and Southwest Asian Late Miocene and Pliocene
981 Hipparionine horses. In: Bernor, R.L., Fahlbusch, V., Mittmann, H.-W. (Eds.), The
982 Evolution of Western Eurasian Neogene Faunas. Columbia University Press, New York, pp.
983 307–338.
984 Bernor, R.L., Tobien, H., Hayek, L.-A.C., Mittmann, H.-W., 1997. *Hippotherium primigenium*
985 (Equidae, Mammalia) from the late Miocene of Höwenegg (Hegau, Germany). Andrias 10,
986 5–230.
987 Bernor, R.L., Kaya, F., Kaakinen, A., Saarinen, J., Fortelius, M., 2021. Old world hipparion
988 evolution, biogeography, climatology and ecology. Earth Sci. Rev. 221, 103784.
989 Bernor, R.L., Cirilli, O., Mittmann, H.-W., 2022. Höwenegg *Hippotherium primigenium*:
990 geological context, cranial and postcranial morphology, palaeoecological and biogeographic
991 importance. Hist. Biol. https://doi.org/10.1080/08912963.2022.2094261

992 Bougeard, S., Dray, S., 2018. Supervised Multiblock Analysis in R with the ade4 Package. J.
993 Stat. Softw. 86, 1–17.
994 Cailleux, F., Van den Hoek Ostende, L.W., Joniak, P., in press. The Late Miocene Erinaceidae
995 and Dimylidae (Eulipotyphla, Mammalia) from the Pannonian Region. J. Paleontol.
996 Cameron, D.W., 1997. A revised systematic scheme for the Eurasian Miocene fossil
997 Hominidae. J, Hum. Evol. 33, 449–477.
998 Cameron, D.W., 1998. Patterns of faciodental sexual dimorphism in *Hispanopithecus*. Z.
999 Morphol. Anthropol. 82, 47–58.
1000 Cameron, D.W., 1999. The single species hypothesis and Hispanopithecus fossils from the
1001 Vallés Penedés Basin, Spain. Z. Morphol. Anthropol. 82, 159–186.
1002 Cameron, D.W., 2004. Hominid Adaptations and Extinctions. University of New South Wales
1003 Press, Sydney.
1004 Casanovas-Vilar, I., Agustí, J., 2007. Ecogeographical stability and climate forcing in the Late
1005 Miocene (Vallesian) rodent record of Spain. Palaeogeogr. Palaeoclimatol. Palaeoecol. 248,
1006 169–189.
1007 Casanovas-Vilar, I., Moyà-Solà, S., Agustí, J., Köhler, M., 2005. The geography of a faunal
1008 turnover: tracking the Vallesian Crisis. In: Elewa, A.T. (Eds.), Migration of Organisms:
1009 Climate, Geography, Ecology. Springer, Heidelberg, pp. 247–301.
1010 Casanovas-Vilar, I., García-Paredes, I., Alba, D.M., van den Hoek Ostende, L., Moyà-Solà, S.,
1011 2010. The European Far West: Miocene mammal isolation, diversity and turnover in the
1012 Iberian Peninsula. J. Biogeogr. 37, 1079–1093.
1013 Casanovas-Vilar, I., Alba, D.M., Garcés, M., Robles, J.M., Moyà-Solà, S., 2011. Updated
1014 chronology for the Miocene hominoid radiation in Western Eurasia. Proc. Natl. Acad. Sci.
1015 USA 108, 5554–5559.

1016 Casanovas-Vilar, I., Van den Hoek Ostende, L., Furió, M., Madern, P.A., 2014. The range and
1017 extent of the Vallesian Crisis (Late Miocene): new prospects based on the micromammal
1018 record from the Vallès-Penedès basin (Catalonia, Spain). J. Iber. Geol. 40, 29–48.
1019 Casanovas-Vilar, I., Almécija, S., Alba, D.M., 2015. Late Miocene flying squirrels from Can
1020 Llobateres 1 (Vallès-Penedès Basin, Catalonia): systematics and paleobiogeography.
1021 Palaeodivers. Palaeoenvir. 95, 353–372.
1022 Casanovas-Vilar, I., Madern, A., Alba, D.M., Cabrera, L., García-Paredes, I., Van den Hoek
1023 Ostende, L.W., DeMiguel, D., Robles, J.M., Furió, M., Van Dam, J., Garcés, M., Angelone,
1024 C., Moyà-Solà, S., 2016a. The Miocene mammal record of the Vallès-Penedès Basin
1025 (Catalonia). C. R. Palevol. 15, 791–812.
1026 Casanovas-Vilar, I., Garcés, M., Van Dam, J., García-Paredes, I., Robles, J.M., Alba, D.M.,
1027 2016b. An updated biostratigraphy for the late Aragonian and Vallesian of the Vallès-
1028 Penedès Basin (Catalonia). Geol. Acta 14, 195–217.
1029 Casanovas-Vilar, I., Torres, J., DeMiguel, D., Alba, D.M., 2018. Introducing: The Vallès-
1030 Penedès Miocene Vertebrates Paleobiodiversity Database. In: The role of NOW in the future
1031 of the past. NOW meeting in Bratislava 9-10 October 2018. Abstract book, pp. 1–2.
1032 Casanovas-Vilar, I., Kimura, Y., Flynn, L.J., Pilbeam, D., Moyà-Solà, S., Alba, D.M., 2019.
1033 Stable isotopes of rodent tooth enamel provide new evidence on Miocene ape environments
1034 in the Vallès-Penedès Basin (Catalonia). In: The Palaeontological Association 63rd Annual
1035 Meeting. 15th-21st December 2019. University of Valencia, Spain. Programme Abstracts
1036 AGM papers, p. 28.
1037 Casanovas-Vilar, I., Kimura, Y., Flynn, L.J., Pilbeam, D., Moyà-Solà, S., Alba, D.M., 2020.
1038 Rodent stable isotopes provide new data on Miocene ape environments in the Siwaliks and
1039 the Vallès-Penedès Basin. Am. J. Phys. Antropol. 171 (S69), 46.

1040 Chessel, D., Dufour, A., Thioulouse, J., 2004. The ade4 Package - I: One-Table Methods. R
1041 News 4, 5–10.
1042 Collyer, M.L., Adams, D.C., 2018. RRPP: An R package for fitting linear models to high-
1043 dimensional data using residual randomization. Methods Ecol. Evol. 9, 1772–1779.
1044 Collyer, M.L., Adams, D.C., 2019. RRPP: Linear model evaluation with randomized residuals
1045 in a permutation orocedure. R package version 1.3.1. https://CRAN.R-
1046 project.org/package=RRPP
1047 Costeur, L., 2005. Cenogram analysis of the Rudabánya mammalian community:
1048 palaeoenvironmental interpretations. Palaeontogr. Ital. 90, 303–307.
1049 Crusafont Pairó, M., 1952. Los jiráfidos fósiles de España. Mem. Com. Inst. Geol. 8, 1–239.
1050 Crusafont Pairó, M., 1958. Nuevo hallazgo del póngido vallesiense *Hispanopithecus*. Bol. Inf.
1051 A.E.P.V. 1, 13–14.
1052 Crusafont Pairó, M., 1965. El desarrollo de los caninos en algunos Driopitécidos del Vallesiense
1053 en Cataluña. Not. Com. Inst. Geol. Min. Esp. 80, 179–191.
1054 Crusafont Pairó, M., 1969. Història de la paleontologia a Sabadell. Joan Sallent Sucr, Sabadell.
1055 Crusafont Pairó, M., Villalta Comella, J.F. de, 1948. El Mioceno continental del Vallés y sus
1056 yacimientos de Vertebrados. Publ. Fund. Bosch Cardellach 3, 7–30.
1057 Crusafont Pairó, M., Hürzeler, J., 1961. Les Pongidés fossiles d'Espagne. C. R. Acad. Sci. Paris
1058 252, 582–584.
1059 Crusafont Pairó, M., Hürzeler, J., 1969. Catálogo comentado de los Póngidos fósiles de España.
1060 Acta Geol. Hisp. 4, 44–48.
1061 Crusafont Pairó, M., Golpe Posse, J.M., 1973. New pongids from the Miocene of Vallès
1062 Penedès Basin (Catalonia, Spain). J. Hum. Evol. 2, 17–24.
1063 Crusafont Pairó, M., Gibert Clols, J., 1974. Nuevos datos sobre el género *Postpalerinaceus* del
1064 Vallesiense. Acta Geol. Hisp 9, 1–3.

de Bonis, L., Abella, J., Merceron, G., Begun, D.R., 2017. A new late Miocene ailuropodine (Giant Panda) from Rudabánya (Northcentral Hungary). Geobios 50, 413–421.

De Bruijn, H., Daams, R., Daxner-Höck, G., Fahlbusch, V., Ginsburg, L., Mein, P., Morales, J., 1992. Report o the RCMNS working group on fossil mammals, Reisensburg 1990. Newsl. Stratigr. 26, 65–118.

DeMiguel, D., Alba, D.M., Moyà-Solà, S., 2014. Dietary specialization during the evolution of Western Eurasian hominoids and the extinction of European great apes. PLoS One 9, e97442.

Domingo, L., Koch, P.L., Hernández Fernández, M., Fox, D.L., Domingo, M.S., Alberdi, M.T., 2013. Late Neogene and early Quaternary paleoenvironmental and paleoclimatic conditions in southwestern Europe: isotopic analyses on mammalian taxa. PLoS One 8, e63739.

Dray, S., Dufour, A., 2007. The ade4 Package: Implementing the Duality Diagram for Ecologists. J. Stat. Softw. 22, 1–20.

Dray, S., Dufour, A., Chessel, D., 2007. The ade4 Package - II: Two-Table and K-Table Methods. R News 7, 47–52.

Eastham, L., Skinner, M., Begun, D.R., 2009. Resolving seasonal stress in the Late Miocene hominoid *Hispanopithecus laietanus* through the analysis of the dental developmental defect linear enamel hypoplasia. J. Vert. Paleontol. 29, 91A.

Eastham, L.C., Feranec, R.S., Begun, D.R., 2016. Stable isotopes show resource partitioning among the early Late Miocene herbivore community at Rudabánya II: Paleoenvironmental implications for the hominoid, *Rudapithecus hungaricus*. Palaeogeogr. Palaeoclimatol. Palaeoecol. 454, 161–174.

Eastham, L.C., Feranec, R.S., Begun, D.R., 2017. Trace element analysis provides insight into the diets of early Late Miocene ungulates from the Rudabánya II locality (Hungary). Geol. Acta 15, 231–243.

1090 Eronen, J.T., Ataabadi, M.M., Micheels, A., Karme, A., Bernor, R.L., Fortelius, M., 2009.
1091 Distribution history and climatic controls of Late Miocene Pikermian chronofauna. Proc.
1092 Natl. Acad. Sci. USA 106, 11867–11871.
1093 Eronen, J.T., Puolamäki, K., Liu, L., Lintulaakso, K., Damuth, J., Janis, C., Fortelius, M.,
1094 2010a. Precipitation and large herbivorous mammals II: application to fossil data. Evol.
1095 Ecol. Res. 12, 235–248.
1096 Eronen, J., Polly, P., Fred, M., Damuth, J., Frank, D., Mosbrugger, V., Scheidegger, C.,
1097 Stenseth, N., Fortelius, M., 2010b. Ecometrics: The traits that bind the past and present
1098 together. Integr. Zool. 5, 88–101.
1099 Eronen, J.T., Puolamäki, K., Liu, L., Lintulaakso, K., Damuth, J., Janis, C., Fortelius, M.,
1100 2010c. Precipitation and large herbivorous mammals I: estimates from present-day
1101 communities. Evol. Ecol. Res. 12, 217–233.
1102 Fortelius, M., Van der Made, J., Bernor, R.L., 1996a. Middle and Late Miocene Suoidea of
1103 Central Europe and the Eastern Mediterranean: Evolution, Biogeography, and Paleoecology.
1104 In: Bernor, R.L., Fahlbusch, V., Mittmann, H.W. (Eds.), The Evolution of Western Eurasian
1105 Neogene Faunas. Columbia University Press, New York, pp. 348–377.
1106 Fortelius, M., Werdelin, L., Andrews, P., Bernor, R.L., Gentry, A., Humphrey, L., Mittmann,
1107 H.-W., Viratana, S., 1996b. Provinciality, diversity, turnover, and paleoecology in land
1108 mammal faunas of the Later Miocene of Western Eurasia. In: Bernor, R.L., Fahlbusch, V.,
1109 Mittmann, H.W. (Eds.), The Evolution of Western Eurasian Neogene Faunas. Columbia
1110 University Press, New York, pp. 414–448.
1111 Fortelius, M., Eronen, J.T., Jernvall, J., Liu, L., Pushkina, D., Rinne, J., Tesakov, A.,
1112 Vislobokova, I., Zhang, Z., Zhou, L., 2002. Fossil mammals resolve regional patterns of
1113 Eurasian climate change during 20 million years. Evol. Ecol. Res. 4, 1005–1016.

1114 Fortelius, M., Žliobaitė, I., Kaya, F., Bibi, F., Bobe, R., Leakey, L., Leakey, M., Patterson, D.,
1115 Rannikko, J., Werdelin, L., 2016. An ecometric analysis of the fossil mammal record of the
1116 Turkana Basin. Phil. Trans. R. Soc. B 371, 20150232.
1117 Furió, M., Prieto, J., Van den Hoek Ostende, L., 2015. Three million years of "Terror-Shrew"
1118 (*Dinosorex*, Eulipotyphla, Mammalia) in the Miocene of the Vallès-Penedès Basin
1119 (Barcelona, Spain). C. R. Palevol. 14, 111–124.
1120 Galbrun, E., Tang, H., Fortelius, M., Žliobaitė, I., 2018. Computational biomes: The ecometrics
1121 of large mammal teeth. Palaeontol. Electron. 21, 21.1.3A.
1122 Garcés, M., Agustí, J., Cabrera, L., Parés, J.M., 1996. Magnetostratigraphy of the Vallesian
1123 (late Miocene) in the Vallès-Penedès Basin (northeast Spain). Earth Plant. Sci. Lett. 142,
1124 381–396.
1125 Golpe-Posse, J.M., 1971. Suiformes del Terciario español y sus yacimientos. Ph.D.
1126 Dissertation, Universidad de Barcelona.
1127 Golpe-Posse, J.M., 1972. Suiformes del terciario español y sus yacimientos (Tesis doctoral-
1128 Resumen) (revisado y reimprimido en Diciembre de 1972). Paleontol. Evol. 2, 1–197.
1129 Golpe Posse, J.M., 1982. Los hispanopitecos (Primates, Pongidae) de los yacimientos del
1130 Vallès Penedès (Cataluña - España). I: Material ya descrito. Bull. Inf. Inst. Paleontol.
1131 Sabadell 14, 63–69.
1132 Golpe Posse, J.M., 1993. Los Hispanopitecos (Primates, Pongidae) de los yacimientos del
1133 Vallès-Penedès (Cataluña, España). II: Descripción del material existente en el Instituto de
1134 Paleontología de Sabadell. Paleontol. Evol. 26–27, 151–224.
1135 Golpe-Posse, J.M., Crusafont Pairó, M., 1982. Caracterización de *Tapirus priscus* Kaup en el
1136 Mioceno superior del Vallés-Penedés. Acta Geol. Hisp. 17, 95–101.
1137 Harrison, T., 1991. Some observations on the Miocene hominoids from Spain. J. Hum. Evol.
1138 20, 515–520.

1139 Heissig, K., 1999. Family Chalicotheriidae. In: Rössner, G.E., Heissig, K. (Eds.), The Miocene
1140 Land Mammals of Europe. Verlag Dr. Friedrich Pfeil, München, pp. 189–192.
1141 Hernández Fernández, M., Salesa, M.J., Sánchez, I.M., Morales, J., 2003. Paleoecología del
1142 género *Anchitherium* von Meyer, 1834 (Equidae, Perissodactyla, Mammalia) en España:
1143 evidencias a partir de las faunas de macromamíferos. Col. Paleontol. 1, 253–280.
1144 Higgins, P., 2018. Isotope ecology from biominerals. In: Croft, D.A., Su, D.F., Simpson, S.W.
1145 (Eds), Methods in Paleoecology. Springer, Cham, pp. 99–120.
1146 Hilgen, F.J., Lourens, L.J., Van Dam, J.A., 2012. The Neogene period. In: Gradstein, F.M.,
1147 Ogg, J.G., Schmitz, M., Ogg, G. (Eds.), The Geologic Time Scale 2012. Elsevier,
1148 Amsterdam, pp. 923–978.
1149 Hunter, J.P., Fortelius, M., 1994. Comparative dental occlusal morphology, facet development,
1150 and microwear in two sympatric species of *Listriodon* (Mammalia: Suidae) from the Middle
1151 Miocene of Western Anatolia (Turkey). J. Vertebr. Paleontol. 14, 105–126.
1152 Iannucci, A., Begun, D.R., 2022. Suidae (Mammalia, Artiodactyla) from the late Miocene
1153 hominoid locality of Alsótelekes (Hungary). Geobios 71, 39–49.
1154 Jackson, S., 2012. Gliding Mammals of the World. CSIRO Publishing, Collingwood.
1155 Jernvall, J., 1995. Mammalian molar cusp patterns: Developmental mechanisms of diversity.
1156 Acta Zool. Fenn. 198, 1–61.
1157 Kassambara, A., Mundt, F., 2020. factoextra: Extract and visualize the results of multivariate
1158 data analyses. R package version 1.0.7. https://CRAN.R-project.org/package=factoextra/
1159 Kaya, F., Bibi, F., Žliobaitė, I., Eronen, J.T., Hui, T., Fortelius, M., 2018. The rise and fall of
1160 the Old World savannah fauna and the origins of the African savannah biome. Nat. Ecol.
1161 Evol. 2, 241–246.
1162 Koch, P.L., 1998. Isotopic reconstruction of past continental environments. Ann. Rev. Earth
1163 Plant. Sci. 26, 573–613.

1164 Kohn, M.J., 2010. Carbon isotope compositions of terrestrial C3 plants as indicators of
1165 (paleo)ecology and (paleo)climate. Proc. Natl. Acad. Sci. USA 107, 19691–19695.
1166 Kohn, M.J., Schoeninger, M.J., Valley, J.W., 1998. Variability in oxygen isotope compositions
1167 of herbivore teeth: reflections of seasonality or developmental physiology? Chem. Geol.
1168 152, 97–112.
1169 Köhler, M., 1993. Skeleton and habitat of recent and fossil rumiants. Münch. Geowiss. Abh. A
1170 25, 1–88.
1171 Liu, L., Puolamaki, K., Eronen, J., Ataabadi, M.M., Hernesniemi, E., Fortelius, M., 2012.
1172 Dental functional traits of mammals resolve productivity in terrestrial ecosystems past and
1173 present. Proc. R. Soc. B 279, 2793–2799.
1174 Lu, X., Ge, D., Xia, L., Zhang, Z., Li, S., Yang, Q., 2013. The evolution and paleobiogeography
1175 of flying squirrels (Sciuridae, Pteromyini) in response to global environmental change. Evol.
1176 Biol. 40, 117–132.
1177 Marmi, J., Casanovas-Vilar, I., Robles, J.M., Moyà-Solà, S., Alba, D.M., 2012. The
1178 paleoenvironment of *Hispanopithecus laietanus* as revealed by paleobotanical evidence
1179 from the Late Miocene of Can Llobateres 1 (Catalonia, Spain). J. Hum. Evol. 62, 412–423.
1180 Mazo, A.V., 1977. Revisión de los mastodontes de España. Ph.D. Dissertation, Universidad
1181 Complutense de Madrid.
1182 Mazo, A.V., Van der Made, J., 2012. Iberian mastodonts: Geographic and stratigraphic
1183 distribution. Quat. Int. 255, 239–256.
1184 McKenzie, S., Sorbelli, L., Cherin, M., Almécija, S., Pina, M., Abella, J., Luján, À.H.,
1185 DeMiguel, D., Alba, D.M., 2023. Earliest Vallesian suid remains from Creu de Conill 20
1186 (Vallès-Penedès Basin, NE Iberian Peninsula). J. Mamm. Evol. 30, 155–212.
1187 Mein, P., 1990. Updating of MN zones. In: Lindsay, E.H., Fahlbush, V., Mein, P. (Eds.),
1188 European Neogene Mammal Chronology. Springer, Boston, pp. 73–90.

1189 Merceron, G., Kaiser, T.M., Kostopoulos, D.S., Schulz, E., 2010. Ruminant diets and the
1190 Miocene extinction of European great apes. Proc. R. Soc. B 277, 3105–3112.
1191 Misas Alcàntara, M., 2022. El paleoambient d'*Hispanopithecus laietanus*: noves dades basades
1192 en l'anàlisi d'isòtops estables de l'esmalt dental dels mamífers herbívors de Can Llobateres.
1193 Graduate Thesis, Universitat Autònoma de Barcelona.
1194 Moyà-Solà, S., 1979. Revisión del género *Dorcatherium* Kaup, 1833 (Mammalia, Ruminantia,
1195 Tragulidae) de las cuencas miocénicas catalanas. Butll. Inf. Inst. Paleontol. Sabadell 11, 55–
1196 59.
1197 Moyà-Solà, S., 1983. Los Boselaphini (Bovidae Mammalia) del Neógeno de la Península
1198 Ibérica. Universidad Autónoma de Barcelona, Barcelona. .
1199 Moyà-Solà, S., Agustí, J., 1990. Bioevents and mammal successions in the Spanish Miocene.
1200 In: Lindsay, E.H., Fahlbusch, V., Mein, P. (Eds.), European Neogene Mammal Chronology.
1201 Plenum Press, New York, pp. 357–373.
1202 Moyà-Solà, S., Köhler, M., 1993. Recent discoveries of *Dryopithecus* shed new light on
1203 evolution of great apes. Nature 365, 543–545.
1204 Moyà-Solà, S., Köhler, M., 1995. New partial cranium of *Dryopithecus* Lartet, 1863
1205 (Hominoidea, Primates) from the upper Miocene of Can Llobateres, Barcelona, Spain. J.
1206 Hum. Evol. 29, 101–139.
1207 Moyà-Solà, S., Köhler, M., 1996. A *Dryopithecus* skeleton and the origins of great-ape
1208 locomotion. Nature 379, 156–159.
1209 Moyà-Solà, S., Pons-Moyà, J., Köhler, M., 1990. Primates catarrinos (Mammalia) del Neógeno
1210 de la península Ibérica. Paleontol. Evol. 23, 41–45.
1211 Moyà-Solà, S., Köhler, M., Alba, D.M., Casanovas-Vilar, I., Galindo, J., Robles, J.M., Cabrera,
1212 L., Garcés, M., Almécija, S., Beamud, E., 2009. First partial face and upper dentition of the
1213 Middle Miocene hominoid Dryopithecus fontani from Abocador de Can Mata (Vallès-

1214 Penedès Basin, Catalonia, NE Spain): taxonomic and phylogenetic implications. Am. J.
1215 Phys. Anthropol. 139, 126–145.
1216 Nagatoshi, K., 1987. Miocene hominoid environments of Europe and Turkey. Palaeogeogr.
1217 Palaeoclimatol. Palaeoecol. 61, 145–154.
1218 Oksanen, O., Žliobaitė, I., Saarinen, J., Lawing, A.M., Fortelius, M., 2019. A Humboldtian
1219 approach to life and climate of the geological past: Estimating palaeotemperature from
1220 dental traits of mammalian communities. J. Biogeogr. 46, 1760–1776.
1221 Peel, M.C., Finlayson, B.L., McMahon, T.A., 2007. Updated world map of the Köppen-Geiger
1222 climate classification. Hydrol. Earth Syst. Sci. 11, 1633–1644.
1223 Pickford, M., 1981. *Parachleuastochoerus* (Mammalia, Suidae). Estud. Geol. 37, 313–320.
1224 Pickford, M., 2014. *Sus valentini* Filhol (1882) from St Gaudens (MN 8–9) France: blighted
1225 from the outset but a key to understanding late Middle Miocene Tetraconodontinae (Suidae,
1226 Mammalia) of Europe. Mainzer Naturwiss. Archiv 51, 167–220.
1227 Pickford, M., 2016. Biochronology of European Miocene Tetraconodontinae (Suidae,
1228 Artiodactyla, Mammalia) flowing from recent revision of the Subfamily. Ann. Naturhist.
1229 Mus. Wien 118, 175–244.
1230 Pickford, M., Pourabrishami, Z., 2013. Deciphering Dinotheriensande deinotheriid diversity.
1231 Palaeobiodivers. Palaeoenviron. 93, 121–150.
1232 Pickford, M., Moyà Solà, S., Mein, P., 1997. A revised phylogeny of Hyracoidea (Mammalia)
1233 based on new specimens of Pliohyracidae from Africa and Europe. N. Jb. Geol. Paläont.
1234 Abh. 205, 265–288.
1235 Pina, M., Alba, D.M., Almécija, S., Fortuny, J., Moyà-Solà, S., 2012. Brief Communication:
1236 Paleobiological inferences on the locomotor repertoire of extinct hominoids based on
1237 femoral neck cortical thickness: the fossil great ape *Hispanopithecus laietanus* as a test-case
1238 study. Am. J. Phys. Anthropol. 149, 142–148.

1239 Pugh, K.D., 2022. Phylogenetic analysis of Middle-Late Miocene apes. J. Hum. Evol. 165,
1240 103140.
1241 R Core Team, 2021. R: A language and environment for statistical computing. R Foundation
1242 for Statistical Computing, Vienna, Austria. https://www.R-project.org/.
1243 Ribot, F., Gibert, J., Harrison, T., 1996. A reinterpretation of the taxonomy of *Dryopithecus*
1244 from Vallès-Penedès, Catalonia (Spain). J. Hum. Evol. 31, 129–141.
1245 Robles, J.M., Abella, J., Madurell-Malapeira, J., Alba, D.M., 2014. Miocene carnivorans from
1246 the Vallès-Penedès Basin. In: Robles, J.M., Miocene carnivorans from the Vallès-Penedès
1247 Basin (NE Iberian Peninsula). Ph.D. Dissertation, Universitat Autònoma de Barcelona, pp.
1248 367–434.
1249 RStudio Team, 2021. RStudio: Integrated Development Environment for R. RStudio, PBC,
1250 Boston. http://www.rstudio.com/
1251 Sanisidro, O., Cantalapiedra, J.L., 2022. The Rhinocerotidae fossil record in the Iberian
1252 Peninsula. Hist. Biol. 34, 1591–1610.
1253 Santafé Llopis, J.V., 1978. Rinocerótidos fósiles de España. Ph.D. Dissertation, Universidad de
1254 Barcelona.
1255 Sanz de Siria Catalán, A., 1993. Datos sobre la paleoclimatología y paleoecología del Neógeno
1256 del Vallès-Penedès según las macrofloras halladas en la Cuenca y zonas próximas. Palentol.
1257 Evol. 26–27, 281–289.
1258 Sanz de Siria Catalán, A., 1994. La evolución de las paleofloras en las cuencas cenozoicas
1259 catalanas. Acta Geol. Hisp. 29, 169–189.
1260 Schlager, S., 2017. Morpho and Rvcg - Shape Analysis in R. In: Zheng, G., Li, S., Szekely, G.
1261 (Eds.), Statistical Shape and Deformation Analysis. Academic Press, London, pp. 217–256.

Sinitsa, M.V., Čermák, S., Kryuchkova, L.Y., 2022. Cranial anatomy of *Csakvaromys bredai* (Rodentia, Sciuridae, Xerinae) and Implications for ground qquirrel evolution and systematics. J. Mamm. Evol. 29, 149–189.

Skinner, M.F., Dupras, T.L., Moyà-Solà, S., 1995. Periodicity of linear enamel hypoplasia among Miocene *Dryopithecus* from Spain. J. Paleopathol. 7, 195–222.

Stefan, V., Levin, S., 2022. plotbiomes: Plot Whittaker biomes with ggplot2. R package version 0.0.0.9001. https://rdrr.io/github/valentinitnelav/plotbiomes/

Susanna, I., Alba, D.M., Almécija, S., Moyà-Solà, S., 2014. The vertebral remains of the late Miocene great ape *Hispanopithecus laietanus* from Can Llobateres 2 (Vallès-Penedès Basin, NE Iberian Peninsula). J. Hum. Evol. 73, 15–34.

Szalay, F., Delson, E., 1979. Evolutionary History of the Primates. Academic Press, New York.

Tallman, M., Almécija, S., Reber, S.L., Alba, D.M., Moyà-Solà, S., 2013. The distal tibia of *Hispanopithecus laietanus*: More evidence for mosaic evolution in Miocene apes. J. Hum. Evol. 62, 319–327.

The NOW Community, 2023. New and Old Worlds Database of Fossil Mammals (NOW). Licensed under CC BY 4.0. https://nowdatabase.org/now/database/ [Accessed May 31, 2023]

Thioulouse, J., Dray, S., Dufour, A., Siberchicot, A., Jombart, T., Pavoine, S., 2018. Multivariate Analysis of Ecological Data with ade4. Springer, New York.

Toivonen, J., Fortelius, M., Žliobaitė, I., 2022. Do species factories exist? Detecting exceptional patterns of evolution in the mammalian fossil record. Proc. R. Soc. B 289, 20212294.

Ungar, P.S., 1996. Dental microwear of European Miocene catarrhines: evidence for diets and tooth use. J. Hum. Evol. 31, 335–366.

Urciuoli, A., Alba, D.M., 2023. Systematics of Miocene apes: State of the art of a neverending controversy. J. Hum. Evol. 175, 103309.

1287 Valenciano, A., Jiangzuo, Q., Wang, S., Li, C., Zhang, X., Ye, J., 2019. First record of *Hoplictis*
1288 (Carnivora, Mustelidae) in East Asia from the Miocene of the Ulungur River Area,
1289 Xianjiang, Northwest China. Acta Geol. Sin. 93, 251–264.
1290 Van Dam, J.A., Krijgsman, W., Abels, H.A., Álvarez-Sierra, M.Á., García-Paredes, I., López-
1291 Guerrero, P., Peláez-Campomanes, P., Ventra, D., 2014. Updated chronology for Middle to
1292 Late Miocene mammal sites of the Daroca área (Calatayud-Montalbán Basin, Spain).
1293 Geobios 47, 325–334.
1294 Van den Hoek Ostende, L.W., Furió, M., 2005. Spain. In: van den Hoek Ostende, L.W.,
1295 Doukas, C.S., Reumer, J.W.F. (Eds.), The Fossil Record of the Eurasian Neogene
1296 Insectivores (Erinaceomorpha, Soricomorpha, Mammalia), Part I. Scripta Geol. Special
1297 Issue 5, 149–284.
1298 Van der Made, J., 1990. Iberian Suoidea. Paleontol. Evol. 23, 83–97.
1299 Van der Made, J., 1996. Listriodontinae (Suidae, Mammalia), their evolution, systematics and
1300 distribution in time and space. Contrib. Tert. Quatern. Geol. 33, 3–254.
1301 Van der Made, J., 1997. Los Suoidea de la Península Ibérica. In: Calvo, J.P., Morales, J. (Eds.),
1302 Avances en el conocimiento del Terciario Ibérico. Cuenca, pp. 109–112.
1303 Van der Made, J., 2010. The pigs and ‘‘Old World peccaries’’ (Suidae and Palaeochoeridae,
1304 Suoidea, Artiodactyla) from the Miocene of Sandelzhausen (southern Germany): phylogeny
1305 and an updated classification of the Hyotheriinae and Palaeochoeridae. Paläontol. Zeits. 84,
1306 43–121.
1307 Van der Made, J., Krakhmalnaya, T., Kubiak, H., 1999. The pig *Propotamochoeurs*
1308 *palaeochoerus* from the upper Miocene of Grytsiv, Ukraine. Estud. Geol. 55, 283–292.
1309 Van der Made, J., Aiglstorfer, M., Böhme, M., 2014. Taxonomic study of the pigs (Suidae,
1310 Mammalia) from the late Middle Miocene of Gratkorn (Austria, Syria). Palaeobiodivers.
1311 Palaeoenviron. 94, 595–617.

1312 Van der Made, J., Choudhary, D., Singh, N.P., Sharma, K.M., Singh, N.A., Patnaik, R., 2022.
1313 *Listriodon dukkar* sp. nov. (Suidae, Artiodactyla, Mammalia) from the late Miocene of
1314 Pasuda (Gujarat, India): the decline and extinction of the Listriodontinae. Paläontol. Zeits.
1315 96, 355–383.
1316 Vermillion, W., Polly, P., Head, J., Eronen, J., Lawing, A., 2018. Ecometrics: A trait-based
1317 approach to paleoclimate and paleoenvironmental reconstruction. In: Croft, D.A., Su, D.F.,
1318 Simpson, S.W. (Eds.), Methods in Paleoecology. Reconstructing Cenozoic Terrestrial
1319 Environments and Ecological Communities. Springer Nature Switzerland, Cham, pp. 373–
1320 394.
1321 Villalta Comella, J.F. de, Crusafont Pairó, M., 1943. Los Vertebrados del Mioceno continental
1322 de la cuenca del Vallés-Penedés (provincia de Barcelona): I. Insectívoros; II. Carnívoros.
1323 Bol. Inst. Geol. Min. España 56, 147–314.
1324 Walter, H., 1979. Vegetation und Klimazonen, 4th ed. Verlag Eugen Ulmer, Stuttgart.
1325 Wickham, H., 2016. ggplot2: Elegant Graphics for Data Analysis. Springer-Verlag, New York.
1326 https://ggplot2.tidyverse.org/
1327 Wickham, H., Hester, J., Chang, W., Bryan, J., 2021. devtools: Tools to Make Developing R
1328 Packages Easier. R package version 2.4.3. https://CRAN.R-project.org/package=devtools/
1329 Whittaker, R., 1975. Communities and Ecosystems, 2nd ed. MacMillan Publishing Co., New
1330 York.
1331 Zanolli, C., Bouchet, F., Fortuny, J., Bernardini, F., Tuniz, C., Alba, D.M., 2023. A
1332 reassessment of the distinctiveness of dryopithecine genera from the Iberian Miocene based
1333 on enamel-dentine junction geometric morphometric analyses. J. Hum. Evol. 177, 103326.
1334 Žliobaitė, I., Rinne, J., Tóth, A., Mechenich, M., Liu, L., Behrensmeyer, A., Fortelius, M., 2016.
1335 Herbivore teeth predict climatic limits in Kenyan ecosystems. Proc. Natl. Acad. Sci. USA
1336 113, 12751–12756.

Žliobaitė, I., Tang, H., Saarinen, J., Fortelius, M., Rinne, J., Rannikko, J., 2018. Dental ecometrics of tropical Africa: linking vegetation types and communities of large plant-eating mammals. Evol. Ecol. Res. 19, 127–147.

Figure captions

Figure 1. Simplified geological map of the Vallès-Penedès Basin showing the location of Can Llobateres 1 (CLL1) and location of the basin within the Iberian Peninsula (inset). Modified from Casanovas-Vilar et al. (2016a: Fig. 1).

Figure 2. Whittaker's diagram with biome classification for Can Llobateres 1 (blue star) based on estimated paleotemperature and paleoprecipitation (Table 5), along with the nine extant localities from Kenyan national parks based on actual temperature and precipitation data (Žliobaitė et al., 2016).

Figure 3. Results of a principal component (PC) analysis based on the seven functional crown type (FCT) variables of 13 extant localities from Kenyan national parks from four different biomes and Can Llobateres 1 (blue star), as depicted by a bivariate plot of PC2 vs. PC1. The percentage of variance summarized by each axis is indicated within parentheses. Vectors represent the loadings of the seven FCT variables (average values) on each axis. Each locality is color-coded according to Whittaker biome classification (see legend). Abbreviations: HYP = hypsodonty; HOD = horizodonty; AL = acute lophs; OL = obtuse lophs; SF = structural fortification; OT = occlusal topography; CM = coronal cementum.

Figure 4. Results of a canonical variate (CV) analysis based on the seven functional crown type (FCT) variables of 18,671 extant localities from five different Whittaker biomes, as depicted by a bivariate plot of CV2 vs. CV1. The percentage of variance summarized by each axis is indicated within parentheses. Vectors represent the loadings of the seven FCT variables (average values) on each axis. Each locality is color-coded according to Whittaker biome classification (see legend). Ellipses represent the 95% confidence interval of each group included a priori. The nine localities from Kenyan national parks classified by this analysis, together with CLL1 (blue star), are also depicted. Kenyan localities: 1 = Shimba Hills; 2 = Kakamega; 3 = Aberdares; 4 = Mt Kenya; 5 = Masaai Mara; 6 = Tsavo; 7 = Nairobi; 8 = Naivasha; 9 = Elgon. Abbreviations: HYP = hypsodonty; HOD = horizodonty; AL = acute lophs; OL = obtuse lophs; SF = structural fortification; OT = occlusal topography; CM = coronal cementum.

Figure 5. Schematic vegetation profile for Can Llobateres 1 based on macrofloral remains recovered from the site. Vegetation zones as well as names of characteristic plants are also indicated. Bold font indicates taxa that have not been recovered at Can Llobateres 1 but occur in other sites of the same basin. A marshy environment populated by reeds (*Phragmites* and *Typha*) is depicted to the left, bordered by a dense riparian evergreen forest with palms (*Sabal*), figtrees (*Ficus*), and laurels (*Cinnamomum*) that would have represented a favorable habitat for hominoids. A more arid, open, and seasonal environment, including areas dominated by leguminous trees, shrubs, and herbaceous plants, is depicted to the right far from the wetlands. Artwork by Roc Olivé.

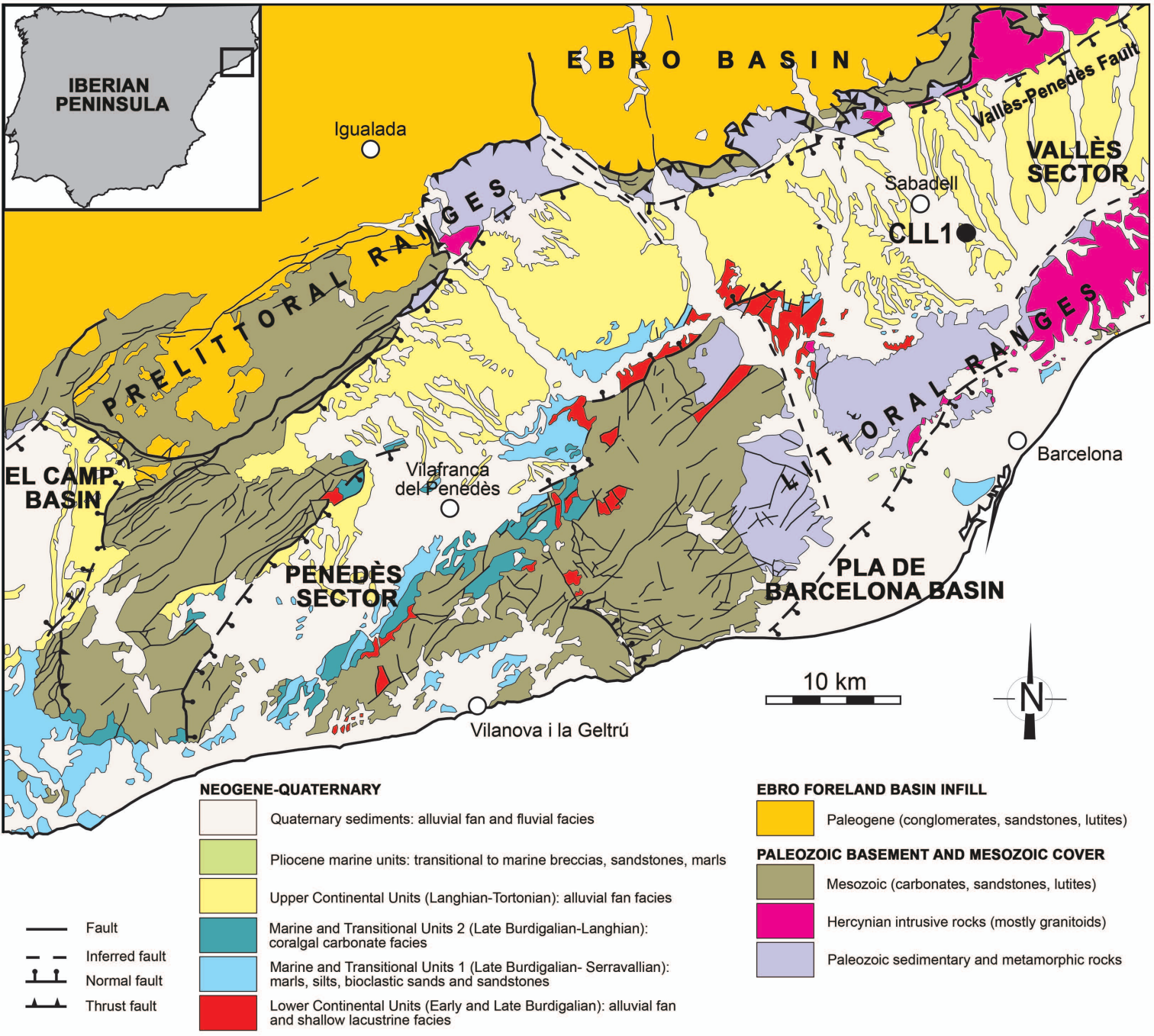
IBERIAN PENINSULA
EBRO BASIN
Igualada
Vallès-Penedès Fault
VALLÈS SECTOR
Sabadell
CLL1
PREL ITTORAL RANGES
LITTORAL RANGES
Barcelona
EL CAMP BASIN
Vilafranca del Penedès
PENEDÈS SECTOR
PLA DE BARCELONA BASIN
10 km
N
Vilanova i la Geltrú
NEOGENE-QUATERNARY
Quaternary sediments: alluvial fan and fluvial facies
Pliocene marine units: transitional to marine breccias, sandstones, marls
Upper Continental Units (Langhian-Tortonian): alluvial fan facies
Marine and Transitional Units 2 (Late Burdigalian-Langhian): coralgal carbonate facies
Marine and Transitional Units 1 (Late Burdigalian- Serravallian): marls, silts, bioclastic sands and sandstones
Lower Continental Units (Early and Late Burdigalian): alluvial fan and shallow lacustrine facies
EBRO FORELAND BASIN INFILL
Paleogene (conglomerates, sandstones, lutites)
PALEOZOIC BASEMENT AND MESOZOIC COVER
Mesozoic (carbonates, sandstones, lutites)
Hercynian intrusive rocks (mostly granitoids)
Paleozoic sedimentary and metamorphic rocks
Fault
Inferred fault
Normal fault
Thrust fault

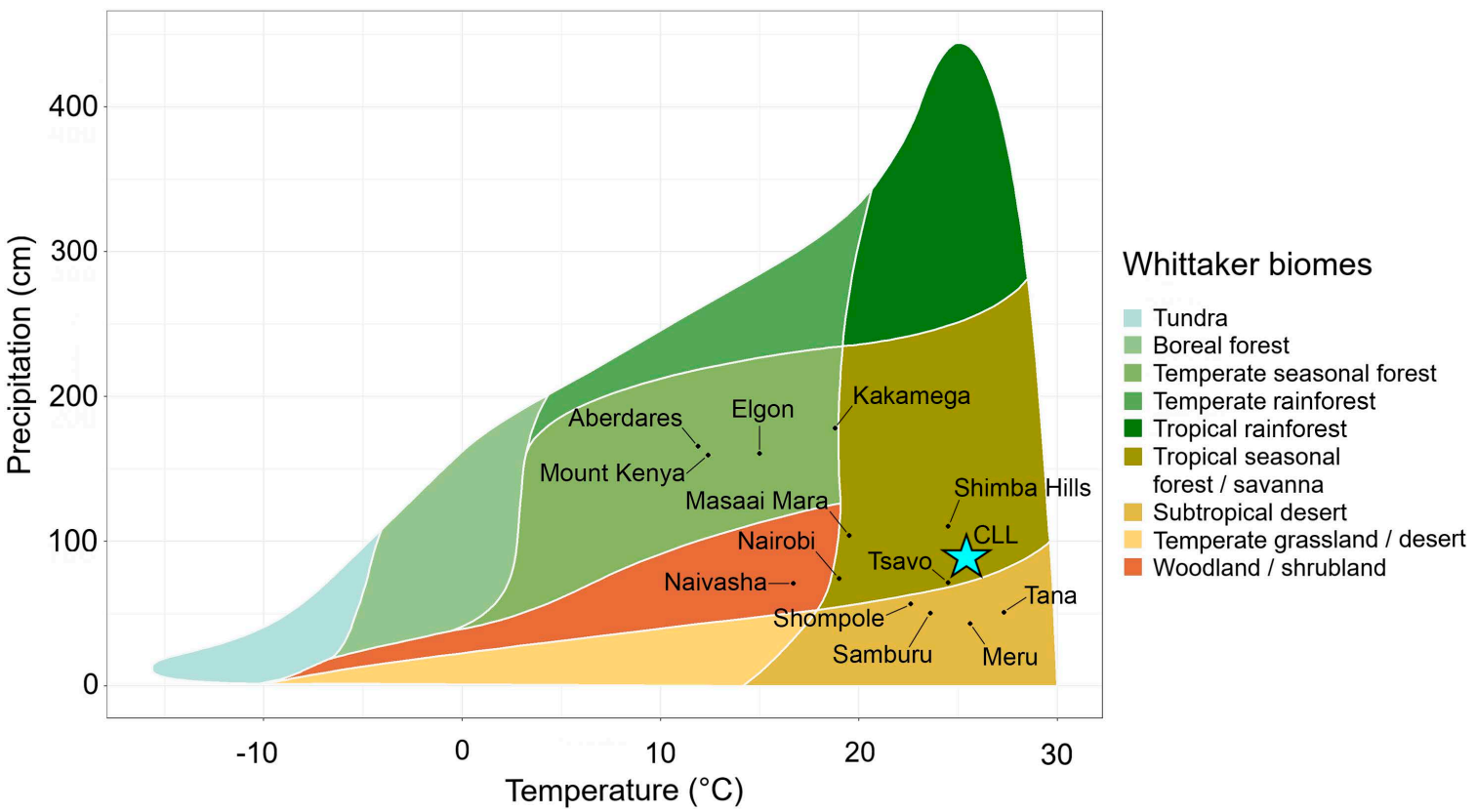
Precipitation (cm)
400
300
200
100
0
-10
0
10
20
30
Temperature (°C)
Aberdares
Elgon
Kakamega
Mount Kenya
Masaai Mara
Shimba Hills
Nairobi
CLL
Tsavo
Naivasha
Tana
Shompole
Samburu
Meru
Whittaker biomes
Tundra
Boreal forest
Temperate seasonal forest
Temperate rainforest
Tropical rainforest
Tropical seasonal forest / savanna
Subtropical desert
Temperate grassland / desert
Woodland / shrubland


AL
CLL
OL
OT
HYP
CM
SF
Shompole
Samburu
Nairobi
Tsavo
Meru
Masaai Mara
Tana
Naivasha
Aberdares
Mount Kenya
Shimba Hills
Kakamega
Elgon
2
0
-2
-4
-4
-2
0
2
4
PC2 (21.34%)
PC1 (56.39%)
Whittaker biomes
Subtropical desert
Temperate seasonal forest
Tropical seasonal forest / savanna
Woodland / shrubland

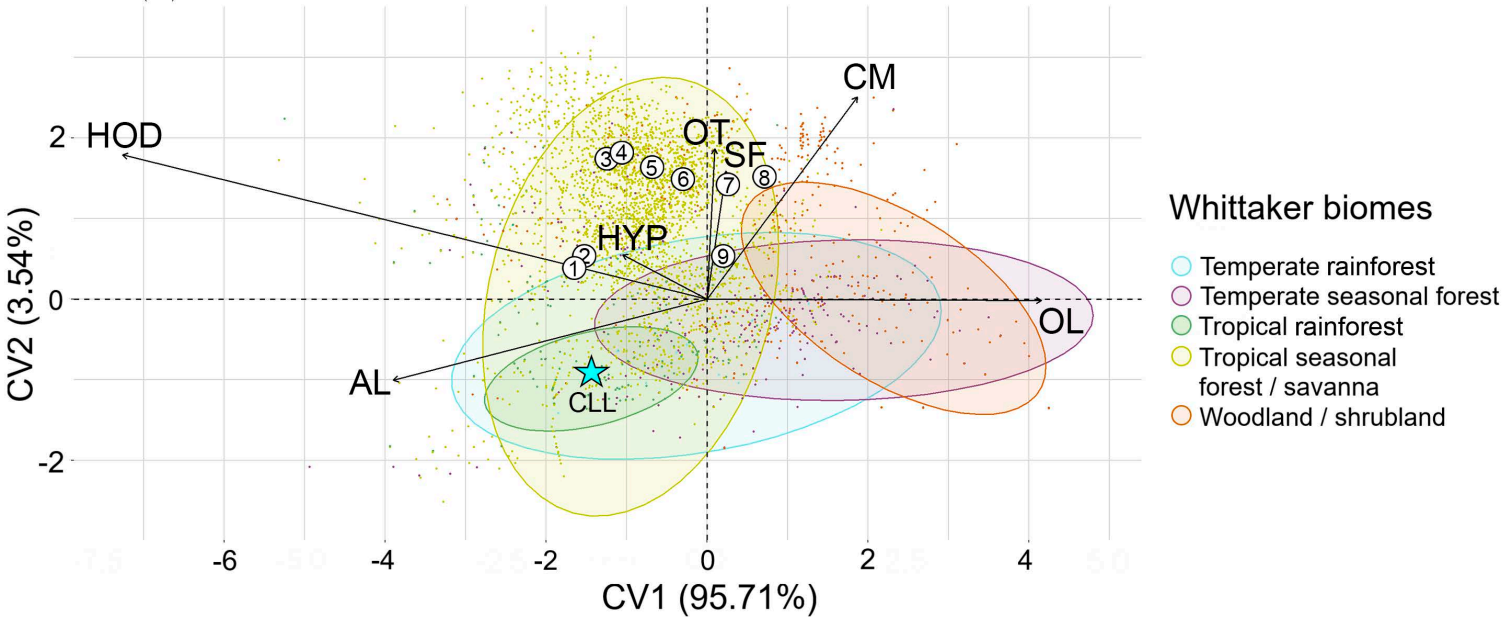
HOD
CM
OT
SF
HYP
OL
AL
CLL
1
2
3
4
5
6
7
8
9
2
0
-2
-6
-4
-2
0
2
4
CV2 (3.54%)
CV1 (95.71%)
Whittaker biomes
Temperate rainforest
Temperate seasonal forest
Tropical rainforest
Tropical seasonal forest / savanna
Woodland / shrubland

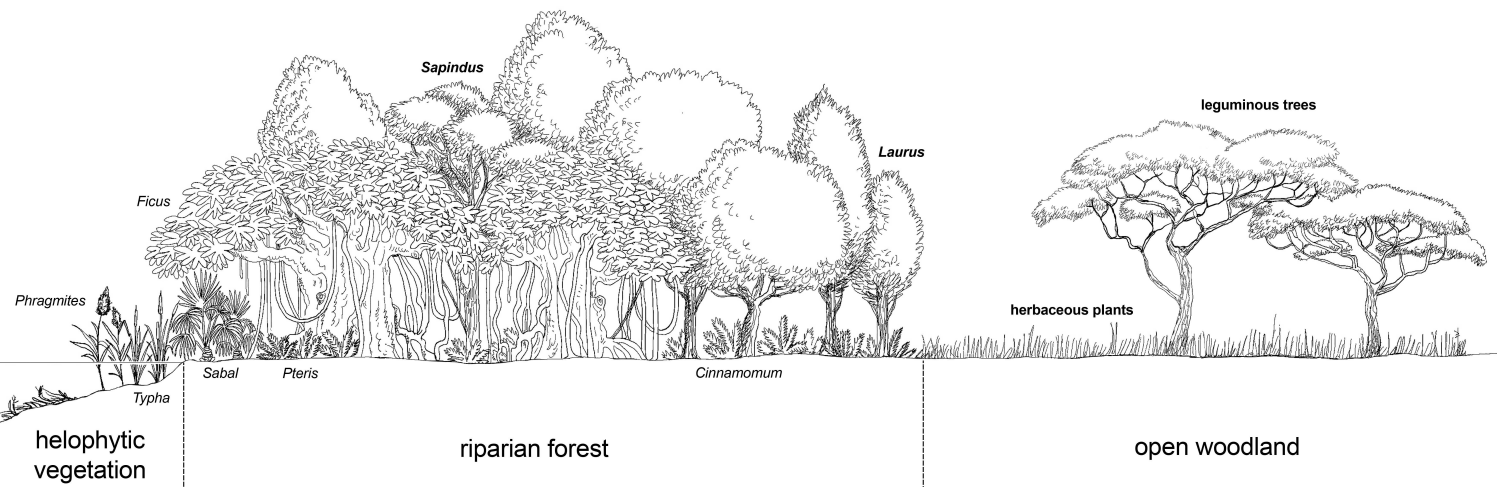
Sapindus
Laurus
Ficus
Phragmites
Sabal
Pteris
Cinnamomum
Typha
leguminous trees
herbaceous plants
helophytic vegetation
riparian forest
open woodland

Table 1

Summary of previous paleoenvironmental reconstructions of Can Llobateres 1 as compared to the present one, including methods, data analyzed, paleoenvironmental inferences, and references.

Reference	Methods and data analyzed	Paleoenvironmental inferences
Nagatoshi (1987)	Qualitative evaluation of fauna and flora	Habitat dominated by fringing forest and open woodland, followed by swamp forest and forest/grassland mosaic, and to a lesser extent parkland and grassland, with river/stream, lake, and marsh water sources
Andrews (1996)	Analysis of community structure using various methods	Classified as a subtropical seasonal forest
Hernández Fernández et al. (2003)	Multivariate analysis of faunal composition	Classified as a deciduous tropical forest with high probability
Costeur (2005)	Cenogram analysis	Considered a tropical forest with very closed and humid conditions
Casanovas-Vilar & Agustí (2007)	Multivariate analysis of the rodent assemblage	Considered a humid warm-temperate evergreen forest
Marmi et al. (2012)	Qualitative evaluation of plant remains	Habitat consisting of a marshy area surrounded by a dense wetland or riparian forest in a warm-temperate climate with high mean

annual temperatures, probably with more open woodlands far from the wetlands

Table 2

Updated list of the mammals from Can Llobateres 1.

Order	Family	Species[a]
Eulipotyphla	Erinaceidae	*Lantanotherium sanmigueli*
Eulipotyphla	Erinaceidae	*Parasorex* sp.
Eulipotyphla	Erinaceidae	cf. *Postpalerinaceus* sp.
Eulipotyphla	Dimylidae	*Plesiodimylus chantrei*
Eulipotyphla	Dimylidae	*Metacordylodon schlosseri*
Eulipotyphla	Talpidae	*Desmanella* sp.
Eulipotyphla	Talpidae	*Talpa vallesiensis*
Eulipotyphla	Talpidae	*Talpa* sp. 2
Eulipotyphla	Heterosoricidae	*Dinosorex grycivensis*
Eulipotyphla	Soricidae	*Miosorex grivensis*
Eulipotyphla	Soricidae	*Lartetium* sp.
Eulipotyphla	Soricidae	*Paenelimnoecus* sp.
Eulipotyphla	Soricidae	*Crusafontina endemica*
Chiroptera	—	Chiroptera indet.
Lagomorpha	Ochotonidae	*Prolagus crusafonti*
Rodentia	Sciuridae	*Csakvaromys bredai*
Rodentia	Sciuridae	*Heteroxerus rubricati*
Rodentia	Sciuridae	*Albanensia* aff. *grimmi*
Rodentia	Sciuridae	*Miopetaurista neogrivensis*
Rodentia	Sciuridae	*Miopetaurista crusafonti*
Rodentia	Sciuridae	*Blackia miocaenica*
Rodentia	Sciuridae	cf. *Pliopetaurista* sp.
Rodentia	Castoridae	*Euroxenomys minutus*
Rodentia	Castoridae	*Chalicomys jaegeri*

Rodentia	Gliridae	*Glirudinus* cf. *undosus*
Rodentia	Gliridae	*Myoglis meini*
Rodentia	Gliridae	*Muscardinus vallesiensis*
Rodentia	Gliridae	*Muscardinus hispanicus*
Rodentia	Gliridae	*Bransatoglis astaracensis*
Rodentia	Gliridae	*Paraglirulus werenfelsi*
Rodentia	Gliridae	*Glirulus lissiensis*
Rodentia	Eomyidae	*Eomyops catalaunicus*
Rodentia	Eomyidae	*Keramidomys pertesunatoi*
Rodentia	Cricetidae	*Eumyarion leemanni*
Rodentia	Cricetidae	*Hispanomys thaleri*
Rodentia	Cricetidae	*Megacricetodon* cf. *minutus*
Rodentia	Cricetidae	*Democricetodon* cf. *nemoralis*
Rodentia	Cricetidae	*Cricetulodon sabadellensis*
Rodentia	Cricetidae	*Anomalomys gaillardi*
Carnivora	Viverridae	*Semigenetta ripolli*
Carnivora	Barbourofelidae	*Albanosmilus jourdani*
Carnivora	Felidae	*Machairodus aphanistus*
Carnivora	Hyaenidae	*Protictitherium crassum*
Carnivora	Amphicyonidae	*Amphicyon* sp.
Carnivora	Amphicyonidae	*Ammitocyon* sp.
Carnivora	Ursidae	*Ursavus brevirhinus*
Carnivora	Ursidae	*Miomaci* sp.
Carnivora	Ursidae	*Indarctos vireti*
Carnivora	Ailuridae	*Protursus simpsoni*
Carnivora	Mephitidae	*Mesomephitis medius*
Carnivora	Mustelidae	*Martes melibulla*

Carnivora	Mustelidae	*Circamustela dechaseauxi*
Carnivora	Mustelidae	*Marcetia santigae*
Carnivora	Mustelidae	*Trochictis narcisoi*
Carnivora	Mustelidae	*Eomellivora fricki*
Carnivora	Mustelidae	*Sabadellictis crusafonti*
Carnivora	Mustelidae	*Trocharion albanense*
Hyracoidea	Pliohyracidae	*Pliohyrax rossignoli*
Proboscidea	Deinotheriidae	***Deinotherium giganteum***
Proboscidea	Gomphotheriidae	***Tetralophodon longirostris***
Perissodactyla	Chalicotheriidae	***Chalicotherium goldfussi***
Perissodactyla	Equidae	***Hippotherium* cf. *primigenium***
Perissodactyla	Rhinocerotidae	***Alicornops simorrense***
Perissodactyla	Rhinocerotidae	**cf. *Aceratherium incisivum***
Perissodactyla	Rhinocerotidae	***Dihoplus* cf. *schleiermacheri***
Perissodactyla	Tapiridae	***Tapirus priscus***
Artiodactyla	Suidae	***Listriodon splendens***
Artiodactyla	Suidae	***Parachleuastochoerus valentini***
Artiodactyla	Suidae	***Parachleuastochoerus crusafonti***
Artiodactyla	Suidae	***Propotamochoerus palaeochoerus***
Artiodactyla	Tragulidae	***Dorcatherium naui***
Artiodactyla	Moschidae	***Micromeryx* aff. *flourensianus***
Artiodactyla	Bovidae	***Miotragocerus pannoniae***
Artiodactyla	Bovidae	***Protragocerus chantrei***
Artiodactyla	Cervidae	***Amphiprox anocerus***
Artiodactyla	Cervidae	**Cervidae indet.**
Artiodactyla	Giraffidae	**Giraffidae indet.**
Primates	Hominidae	***Hispanopithecus laietanus***

[a] Taxa included in the ecometric analyses are in bold.

Table 3

Definition and scoring of functional crown type variables following Žliobaitė et al. (2016).

Variable	Abbreviation	Definition	Scoring			
			0	1	2	3
Hypsodonty	HYP	Height of a tooth crown relative to its length[a]		Brachyodont	Mesodont	Hypsodont
Horizodonty	HOD	Length of the functional occlusal surface (number of main cusp pairs along the mesiodistal axis)[b]		Brachyhorizodont	Mesohorizodont	Hypsohorizodont
Acute lophs	AL	Sloped linear structures typically having straight edges	Absent	Present		
Obtuse lophs	OL	Nonsloped linear structures that typically have curved edges	Absent	Present		
Structural fortification of cusps	SF	Structures that strengthen and reinforce the cusps (usually by differential thickness of enamel)	Absent	Present		

Occlusal topography	OT	Lack (flat) or presence (non-flat) of occlusal raised elements such as cusps[c]	With raised elements	Flat
Coronal cementum	CM	Presence or absence of thickened cementum in the crown, supporting its strength and durability	Absent or very thin	Thick coating

[a] Hypsodonty categories (Fortelius et al., 2002; Žliobaitė et al., 2016; Galbrun et al., 2018): brachyodont = lower than long (<0.8); mesodont = approximately as tall as long (0.8–1.2); hypsodont = taller than long (>1.2).

[b] Horizodonty categories (Žliobaitė et al., 2016): brachyhorizodont = 1–2 cusp pairs; mesohorizodont = 3 cusp pairs; hypsohorizodont = more than 3 cusp pairs.

[c] Lophodont teeth can be flat or non-flat.

Table 4

Scoring of the functional crown types variables for the species of herbivorous large mammals recorded from Can Llobateres 1 (based on the M^2) and average value computed for each variable.[a]

Species	HYP	HOD	AL	OL	SF	OT	CM
Deinotherium giganteum	1	1	1	0	0	0	0
Tetralophodon longirostris	1	3	0	1	0	0	0
Chalicotherium goldfussi	1	1	1	0	0	0	0
Hippotherium cf. *primigenium*	3	1	0	1	0	1	1
Alicornops simorrense	1	1	1	1	0	0	0
cf. *Aceratherium incisivum*	1	1	1	1	0	0	0
Dihoplus cf. *schleiermacheri*	1	1	1	1	0	0	0
Tapirus priscus	1	1	1	0	0	0	0
Listriodon splendens	1	1	1	0	0	0	0
Parahcleuastochoerus valentini	1	1	0	0	1	0	0
Parachleuastochoerus crusafonti	1	1	0	0	0	0	0
Propotamochoerus palaeochoerus	1	1	0	0	1	0	0
Dorcatherium naui	1	1	0	1	0	0	0
Micromeryx aff. *flourensianus*	1	1	0	1	0	0	0
Miotragocerus pannoniae	2	1	0	1	0	0	0
Protragocerus chantrei	1	1	0	1	0	0	0
Amphiprox anocerus	1	1	0	1	0	0	0
Cervidae indet.	1	1	0	1	0	0	0
Giraffidae indet.	1	1	0	1	0	0	0

Hispanopithecus laietanus	1	1	0	0	0	0	0
Mean	1.150	1.100	0.350	0.600	0.100	0.050	0.050

Abbreviations: HYP = hypsodonty; HOD = horizodonty; AL = acute lophs; OL = obtuse or basin-like lophs; SF = structural fortification of cusps; OT = occlusal topography; CM = coronal cementum.

[a] The scoring protocol of Žliobaitė et al. (2016) is followed (no acute lophs are scored for selenodonts). See the Materials and methods for details about the meaning of each score.

Table 5

Estimates of 23 environmental variables for Can Llobateres 1 (CLL1) based on the regressions published by Žliobaitė et al. (2016)[a] and the functional crown type variables computed in this study for CLL1 (Table 4).

Paleoenvironmental variable	Estimates for CLL1
Mean annual precipitation (MAP)[b]	**881 mm**
Driest month over year	136 mm
Driest place over year	974 mm
Wettest month over year	2119 mm
Wettest place over year	816 mm
Average annual NPP	1352 g C/m^2
Coldest and driest month over year	174 g C/m^2
Coldest days with driest place	1090 g C/m^2
Coldest days with driest month	182 g C/m^2
Coldest month driest place over year	1257 g C/m^2
Average NDVI	0.91
Global minimum over 9 yr	0.60
Average over yearly minimums	0.67
Minimum over yearly averages	0.68
Average over monthly minimums	0.85
Minimum over monthly minimums	0.74
Mean annual temperature (MAT)[b]	**25 °C**
Coldest month over year	24 °C
Average over coldest days of months	17 °C
Minimum over coldest days of months	17 °C
Hottest month over year	27 °C
Average over hottest days of months	30 °C

Maximum over hottest days of months	34 °C

Abbreviation: NDVI = normalized difference vegetation index; NPP = net primary productivity.

[a] See SOM Table S1 for the parameters of Žliobaitė et al.'s (2016: Table 2) regressions. The variables used in Whittaker's biome attribution are bolded.

[b] These variables were termed annual precipitation and average temperature in Žliobaitė et al. (2016).

Table 6

Summary classification results (in %) for the selected 18,671 extant localities from five Whittaker biomes based on the canonical variate analysis of seven functional crown type variables with cross-validation.[a]

	Temperate rainforest	Temperate seasonal forest	Tropical rainforest	Tropical seasonal forest/savanna	Woodland/shrubland
Temperate rainforest	**43.2**	4.9	29.6	9.9	12.4
Temperate seasonal forest	22.4	**23.7**	7.9	5.6	40.4
Tropical rainforest	8.8	0.3	**81.5**	9.4	0.1
Tropical seasonal forest/savanna	14.0	1.9	42.1	**41.7**	0.4
Woodland/shrubland	6.5	16.4	0.7	3.6	**72.8**

[a] Correct classification percentages after cross-validation are bolded.

Table 7

Posterior probabilities and typicality probabilities for each Whittaker's biome based on the canonical variate analysis of functional crown type variables for Can Llobateres 1 and nine extant localities from Kenyan national parks (Žliobaitė et al., 2016).

Posterior probabilities					
Locality	Temperate rainforest	Temperate seasonal forest	Tropical rainforest	Tropical seasonal forest/savanna	Woodland/shrubland
Aberdares	0.087	0.011	0.094	**0.806**	0.002
Elgon	0.245	0.210	0.092	**0.353**	0.100
Kakamega	0.116	0.009	0.230	**0.644**	0.001
Masaai Mara	0.157	0.025	0.099	**0.705**	0.013
Mt Kenya	0.090	0.013	0.096	**0.796**	0.004
Nairobi	0.228	0.104	0.067	**0.419**	0.181
Naivasha	0.187	0.195	0.025	0.222	**0.371**
Shompole	0.126	0.004	0.316	**0.553**	0.000
Tsavo	0.209	0.054	0.091	**0.607**	0.039
Can Llobateres 1	0.062	0.005	**0.629**	0.304	0.001
Typicality probabilities					

Locality	Temperate rainforest	Temperate seasonal forest	Tropical rainforest	Tropical seasonal forest/savanna	Woodland/shrubland
Aberdares	0.081	0.015	0.087	**0.429**	0.003
Elgon	0.547	0.497	0.286	**0.675**	0.302
Kakamega	0.094	0.011	0.160	**0.340**	0.001
Masaai Mara	0.209	0.049	0.147	**0.579**	0.028
Mt Kenya	0.123	0.025	0.129	**0.575**	0.010
Nairobi	0.029	0.015	0.010	**0.048**	0.024
Naivasha	0.064	0.066	0.012	0.074	**0.111**
Shompole	0.414	0.028	0.717	**0.912**	0.005
Tsavo	0.230	0.080	0.122	**0.482**	0.062
Can Llobateres 1	0.100	0.013	**0.534**	0.333	0.002

[a] The highest probabilities for each locality are bolded.

Table 8

Whittaker's biome classification of Can Llobateres 1 and nine extant localities from Kenyan national parks (Žliobaitė et al., 2016) based on temperature and precipitation (TP) and a canonical variate analysis (CVA) of functional crown type variables.[a]

Locality	Whittaker's biome (TP)	Whittaker's biome (CVA)
Aberdares	Temperate seasonal forest	Tropical seasonal forest/savanna
Elgon	Temperate seasonal forest	Tropical seasonal forest/savanna
Kakamega	Temperate seasonal forest	Tropical seasonal forest/savanna
Masaai Mara	**Tropical seasonal forest/savanna**	**Tropical seasonal forest/savanna**
Mt Kenya	Temperate seasonal forest	Tropical seasonal forest/savanna
Nairobi	**Tropical seasonal forest/savanna**	**Tropical seasonal forest/savanna**
Naivasha	**Woodland/shrubland**	**Woodland/shrubland**
Shompole	**Tropical seasonal forest/savanna**	**Tropical seasonal forest/savanna**
Tsavo	**Tropical seasonal forest/savanna**	**Tropical seasonal forest/savanna**
Can Llobateres 1	Tropical seasonal forest/savanna	Tropical rainforest

[a] Biome names are bolded for those localities in which both methods yield the same biome attributions.

Supplementary Online Material (SOM):

Paleoenvironmental inferences on the Late Miocene hominoid-bearing site of Can Llobateres (NE Iberian Peninsula): An ecometric approach based on functional dental traits

Sara G. Arranz[a,*], Isaac Casanovas-Vilar[a], Indrė Žliobaitė[b,c], Juan Abella[d,a,e], Chiara Angelone[f,g], Beatriz Azanza[h], Raymond Bernor[i,j], Omar Cirilli[i,k], Daniel DeMiguel[h,l,a], Marc Furió[m,a], Luca Pandolfi[n], Josep M. Robles[a], Israel M. Sánchez[a], Lars W. van den Hoek Ostende[o], David M. Alba[a,*]

[a] *Institut Català de Paleontologia Miquel Crusafont, Universitat Autònoma de Barcelona, c/ Columnes s/n, 08193 Cerdanyola del Vallès, Barcelona, Spain*

[b] *Department of Computer Science, University of Helsinki, P.O. Box 68, 00014 Helsinky, Finland*

[c] *Department of Geosciences and Geography, University of Helsinki, P.O. Box 64, 00014 Helsinky, Finland*

[d] *Grup d'Investigació en Paleontologia de Vertebrats del Cenozoic (PVC-GIUV), Departament de Botànica i Geologia, Universitat de València, 46100 Burjassot, València, Spain*

[e] *Instituto Nacional de Biodiversidad (INABIO), Pje. Rumipamba N. 341 y Av. de los Shyris (Parque La Carolina), Quito, Ecuador*

[f] *Dipartimento di Scienze, Universita` degli Studi Roma Tre, 00146 Roma, Italy*

[g] *Key Laboratory of Vertebrate Evolution and Human Origins, Institute of Vertebrate Paleontology and Paleoanthropology, Chinese Academy of Sciences, 100044 Beijing, China*

[h] *Departamento de Ciencias de la Tierra, and Instituto Universitario de Investigación en Ciencias Ambientales de Aragón (IUCA), Universidad de Zaragoza, 50009, Zaragoza, Spain*

[i] *College of Medicine, Department of Anatomy, Laboratory of Evolutionary Biology, Howard University, 520 W St. N.W., 20059, Washington D.C., USA*

[j] *Human Origins Program, Department of Anthropology, National Museum of Natural History, Smithsonian Institution, 20013, Washington DC, USA*

[k] *Earth Sciences Department, Paleo[Fab]Lab, Università degli Studi di Firenze, via G. La Pira 4, I-50121, Firenze, Italy*

[l] *ARAID foundation, 50018, Zaragoza, Spain*

[m] *Serra Húnter Fellow, Departament de Geologia, Universitat Autònoma de Barcelona, Campuys de la UAB, 08193 Cerdanyola del Vallès,, Barcelona, Spain*

[n] *Dipartimento di Scienze, Università della Basilicata, via dell'Ateneo Lucano, 10, 85100, Potenza, Italy*

[o] *Naturalis Biodiversity Center, Darwinweg 2, 2333 CR Leiden, The Netherlands*

***Corresponding authors.**

E-mail addresses: sara.arranz@icp.cat (S.G. Arranz); david.alba@icp.cat (D.M. Alba).

SOM Table S1

Parameters of the regressions reported by Žliobaitė et al. (2016: Table 2) to estimate 23 environmental variables based on average values of functional crown type variables for a given locality.

Prediction target	Regression coeficients								Accuracy		Description of the prediction target
	Intercept	HYP	HOD	AL	OL	SF	OT	CM	R^2	R^2*	
PREC	-1765		2156			3969	-2441		0.68	0.38	Annual precipitation
PREC_MIN	-1688		1481			2325	-762		0.66	0.36	Driest month over year
PREC_low	966					1456	-2444	-310	0.76	0.53	Driest place over year
PREC_MAX	1486			775		3741	-245		0.27	-0.01	Wettest month over year
PREC_high	-3561		3553			5339	-1300		0.56	0.24	Wettest place over year
NPP	1179					2907	-2331	-15	0.71	0.51	Average annual NPP
NPP_MIN_MIN	-2447		2049			4112	-876		0.66	0.40	Coldest and driest month over year
NPP_low_low	972	25				2639		-3495	0.77	0.65	Coldest days with driest place
NPP_low_MIN	-2265		1896			4071	-914		0.67	0.40	Coldest days with driest month
NPP_MIN_low	1162					2307	-2041	-667	0.74	0.55	Coldest month driest place over year
NDVI	0.337			1.429		0.879	-0.374		0.59	0.26	Average NDVI
NDVI_MIN9y	0.410			0.789	-0.098		-0.479		0.50	-0.08	Global minimum over 9 y
NDVI_low1y	0.419			0.721		0.396	-0.869		0.66	0.26	Average over yearly minimums

NDVI_low1y_MIN	0.314		0.846		0.88	-0.378	0.51	0.20	Minimum over yearly averages
NDVI_low	0.347		1.281		0.818	-0.447	0.59	0.27	Average over monthly minimums
NDVI_low_MIN	0.300		0.986		0.887	-0.63	0.67	0.33	Minimum over monthly minimums
TEMP	43.9			-23.0	-53.5	13.1	0.57	-0.05	Average temperature
TEMP_MIN	44.3			-24.7	-56.4	11.6	0.60	0.04	Coldest month over year
TEMP_low	28.6			-13.6	-35.7	7.2	0.37	-0.37	Average over coldest days of months
TEMP_low_MIN	28.3			-13.4	-37.8	2.8	0.37	-0.33	Minimum over coldest days of months
TEMP_MAX	44.7			-22.5	-52.3	13.7	0.54	-0.12	Hottest month over year
TEMP_high	55.2		-16.8	-20.7	-67.9		0.62	0.23	Average over hottest days of months
TEMP_high_MAX	54.0		-8.9	-18.0	-62.9		0.57	0.19	Maximum over hottest days of months

Abbreviations: HYP = hypsodonty; HOD = horizodonty; AL = acute lophs; OL = obtuse or basin-like lophs; SF = structural fortification of cusps; OT = occlusal topography; CM = coronal cementum; R^2 = goodness of fit (model calibration accuracy); R^2* = predictive power (accuracy measured via cross-validation).

SOM References

Žliobaitė, I., Rinne, J., Tóth, A., Mechenich, M., Liu, L., Behrensmeyer, A., Fortelius, M., 2016. Herbivore teeth predict climatic limits in Kenyan ecosystems. Proc. Natl. Acad. Sci. USA 113, 12751–12756.